Chemical Geology 495 (2018) 36–49

Contents lists available at ScienceDirect

Chemical Geology

journal homepage: www.elsevier.com/locate/chemgeo

Sr and Nd isotopic compositions of individual olivine-hosted melt inclusions from Hawai'i and Samoa: Implications for the origin of isotopic heterogeneity in melt inclusions from OIB lavas

A.A. Reinhard[a,*], M.G. Jackson[a], J.M. Koornneef[b], E.F. Rose-Koga[c], J. Blusztajn[d], J.G. Konter[e], K.T. Koga[c], P.J. Wallace[f], J. Harvey[g]

[a] University of Calfornia Santa Barbara, Department of Earth Science, Santa Barbara, CA, United States of America
[b] Vrije Universiteit Amsterdam, Faculty of Science, Amsterdam, the Netherlands
[c] Université Clermont Auvergne, CNRS, IRD Laboratoire Magmas et Volcans, OPGC, Clermont-Ferrand, France
[d] Woods Hole Oceanographic Institution, Woods Hole, MA, United States of America
[e] University of Hawai'i Manoa, Department of Geology and Geophysics, Honolulu, HI, United States of America
[f] University of Oregon, Department of Earth Sciences, Eugene, OR, United States of America
[g] University of Leeds, School of Earth and Environment, Leeds, UK

ARTICLE INFO

Editor: Catherine Chauvel

Keywords:
Melt inclusions
$^{87}\mathrm{Sr}/^{86}\mathrm{Sr}$
$^{143}\mathrm{Nd}/^{144}\mathrm{Nd}$
Mantle geochemistry
TIMS

ABSTRACT

Geochemical investigations of mantle heterogeneity as sampled by ocean island basalts (OIB) have long relied on isotopic analyses of whole rock lavas. However recent work has shown that significant isotopic disequilibrium can exist between the phases (groundmass and phenocrysts) of a single OIB lava. In this study, we target individual olivine-hosted melt inclusions from two samples—one Samoan and one Hawai'ian—with melt inclusion $^{87}\mathrm{Sr}/^{86}\mathrm{Sr}$ heterogeneity previously measured using laser ablation inductively coupled plasma mass spectrometry (LA-ICP-MS). We report $^{87}\mathrm{Sr}/^{86}\mathrm{Sr}$ and $^{143}\mathrm{Nd}/^{144}\mathrm{Nd}$ in individual melt inclusions analyzed by thermal ionization mass spectrometry (TIMS). In melt inclusions from Samoan sample AVON3-71-2, we find highly heterogeneous (935 ppm) $^{87}\mathrm{Sr}/^{86}\mathrm{Sr}$ (0.705193–0.705853, $N = 6$), consistent with previously identified $^{87}\mathrm{Sr}/^{86}\mathrm{Sr}$ heterogeneity (~2030 ppm) by laser ablation multi-collector ICP-MS (0.70459–0.70602, $N = 12$). In contrast, we find comparatively little (251 ppm) $^{87}\mathrm{Sr}/^{86}\mathrm{Sr}$ heterogeneity (0.703761–0.703938, $N = 9$) in olivine-hosted melt inclusions contained in a Hawaiian scoria clast from the Pu'u Wahi eruption (Mauna Loa). This result contrasts with a previous measurements by single-collector LA-ICP-MS that found highly heterogeneous (~8500 ppm) $^{87}\mathrm{Sr}/^{86}\mathrm{Sr}$ in olivine-hosted melt inclusions from the same eruption (0.7021–0.7081, $N = 137$). In both the AVON3-71-2 and Pu'u Wahi melt inclusions, $^{143}\mathrm{Nd}/^{144}\mathrm{Nd}$ is indistinguishable from their respective whole rock $^{143}\mathrm{Nd}/^{144}\mathrm{Nd}$ values. The isotopic measurements on the melt inclusions are paired with major and trace element concentrations to investigate the mechanisms generating $^{87}\mathrm{Sr}/^{86}\mathrm{Sr}$ variability in melt inclusions. The lack of significant $^{87}\mathrm{Sr}/^{86}\mathrm{Sr}$ variability in the Hawai'ian melt inclusions (only 251 ppm) from Pu'u Wahi suggests a relatively simple magmatic history. In contrast, for the Samoan melt inclusions, we present evidence that supports the mixing of isotopically-heterogeneous mantle-derived melts as the mechanism generating the observed $^{87}\mathrm{Sr}/^{86}\mathrm{Sr}$ and trace element variability in the melt inclusions from AVON3-71-2. However, brine interaction appears to have increased the Cl concentrations of some of the Samoan inclusions without significantly modifying the $^{87}\mathrm{Sr}/^{86}\mathrm{Sr}$ or the other elemental budgets examined in this study.

1. Introduction

Geochemical studies have dominantly relied on analyses of whole-rock lavas to infer the composition of the mantle beneath ocean island hotspots (e.g., Gast et al., 1964; Hofmann and White, 1982; White, 1985; Zindler and Hart, 1986; Sun and McDonough, 1989; Carlson, 1994; Hofmann, 1997; White, 2010, 2015a, 2015b; Stracke, 2016). However, small blebs of melt trapped in growing magmatic phenocrysts at depth—referred to as melt inclusions—have been shown to host extreme geochemical heterogeneity that is not observed in analyses of individual whole-rock lavas. Melt inclusions from a single lava can host heterogeneous Pb (e.g., Saal et al., 1998, 2005; Yurimoto et al., 2004; Maclennan, 2008; Sakyi et al.,

---

* Corresponding author.
E-mail address: reinhard@umail.ucsb.edu (A.A. Reinhard).

https://doi.org/10.1016/j.chemgeo.2018.07.034
Received 3 December 2017; Received in revised form 17 July 2018; Accepted 31 July 2018

2012; Borisova et al., 2014; Cabral et al., 2014; Rose-Koga et al., 2012, 2017) and Sr (Jackson and Hart, 2006; Harlou et al., 2009; Sobolev et al., 2011) isotopic compositions that span much of the variability observed in oceanic lavas globally. Despite their volumetrically minor contribution to the whole rock lava, the isotopic diversity preserved in melt inclusions provides important information about mantle melting and the processes that operate in magma chambers. The origin of the chemical and isotopic diversity in melt inclusions remains a source of debate but has most often been attributed to either assimilation of oceanic crust or mixing of isotopically heterogeneous mantle melts (e.g., Sobolev and Shimizu, 1993; Gurenko and Chaussidon, 1995; Kent et al., 1999a, 1999b; Sobolev et al., 2000; Lassiter et al., 2002; Maclennan et al., 2003a, 2003b; Danyushevsky et al., 2003, 2004; Sobolev et al., 2011; Cabral et al., 2013).

Only a handful of studies have examined Sr isotopic compositions of olivine-hosted melt inclusions from ocean island basalt (OIB) lavas. Jackson and Hart (2006) were the first to target individual olivine-hosted melt inclusions for Sr isotopic analysis, utilizing laser ablation multi-collector inductively coupled plasma mass spectrometry (LA-MC-ICP-MS) to analyze melt inclusions from Samoan picrites. They found $^{87}Sr/^{86}Sr$ variability as large as 3400 ppm within olivine-hosted melt inclusions from a single basalt. This result was reinforced by the work of Harlou et al. (2009), who employed micro-milling, traditional column chemistry (to separate Sr), and thermal ionization mass spectrometry (TIMS) to analyze the $^{87}Sr/^{86}Sr$ of individual olivine-hosted melt inclusions. Harlou et al. (2009) found even greater $^{87}Sr/^{86}Sr$ heterogeneity ($>$ 6000 ppm) than Jackson and Hart (2006) in olivine-hosted melt inclusions from an Icelandic lava. A more recent single-collector LA-ICP-MS study (Sobolev et al., 2011) reported remarkable $^{87}Sr/^{86}Sr$ variability (0.7021 to 0.7081, or ~8500 ppm) in olivine-hosted melt inclusions from a single olivine-rich scoria clast (the “Pu'u Wahi” eruption) from Mauna Loa, Hawai'i. These studies collectively appear to demonstrate that intra-basalt Sr isotopic heterogeneity exists within olivine-hosted melt inclusion populations in OIB from several localities, and that whole-rock $^{87}Sr/^{86}Sr$ analyses do not accurately capture the full isotopic variability of the melts that contribute to the geochemical signature of a basalt.

Complementary studies have shown that intra-lava Sr-isotopic variability also exists in other phases in mid-ocean ridge basalts (MORB) (Bryce and DePaolo, 2004) and OIB. In Samoan lavas significant isotopic disequilibrium has been observed between whole rocks and clinopyroxene separates (as large as ~3100 ppm for $^{87}Sr/^{86}Sr$ and 160 ppm for $^{143}Nd/^{144}Nd$; (Jackson et al., 2009)). More recently Reinhard et al. (2016) observed $^{87}Sr/^{86}Sr$ disequilibrium as large as 1947 ppm (in Samoan lava AVON3-78-1) between aggregated olivines and host whole rocks, confirming Jackson and Hart's (2006) observation that melt inclusions hosted in olivines are not always in isotopic equilibrium with the host lava. In summary, there is overwhelming evidence for radiogenic isotopic variability preserved in the various components (clinopyroxene, olivine, melt inclusions) hosted in fresh, young OIB lavas. However, the mechanisms generating the Sr isotopic disequilibrium remain poorly understood. The three studies reporting $^{87}Sr/^{86}Sr$ heterogeneity in melt inclusions (Jackson and Hart, 2006; Harlou et al., 2009; Sobolev et al., 2011) provide no consensus on the mechanisms responsible for the variability.

More recently, Koornneef et al. (2015) utilized high precision isotopic analyses by TIMS in individual olivine-hosted melt inclusions from Italian Neogene – Quaternary lavas and found significant $^{87}Sr/^{86}Sr$ and $^{143}Nd/^{144}Nd$ heterogeneity between melt inclusions from single lavas. Based on these successful measurements of $^{87}Sr/^{86}Sr$ and $^{143}Nd/^{144}Nd$ in individual melt inclusions from enriched arc lavas by Koornneef et al. (2015), we apply the same high precision TIMS technique to melt inclusions from OIB lavas which transit the thinner, less enriched oceanic crust. Here we present the first $^{87}Sr/^{86}Sr$ and $^{143}Nd/^{144}Nd$ measurements by TIMS, paired with major, trace, and volatile-element analyses, from individual olivine-hosted melt inclusions erupted at two oceanic hotspots. This study targets olivine-hosted melt inclusions from one Hawai'ian scoria clast (Sobolev et al., 2011; Wallace et al., 2015) and one Samoan lava (Jackson and Hart, 2006), both of which were targeted for Sr-isotopic analyses on olivine-hosted melt inclusions by LA-ICP-MS in previous studies. We use a different analytical approach—wet chemistry and isotopic analysis by TIMS—to obtain precise Sr and Nd isotopic data on melt inclusions from the same Samoan lava and a clast from the same Mauna Loa eruption sampled by Sobolev et al. (2011). An important advantage of the TIMS analytical technique is that it does not suffer from the same uncertainties in correcting for isobaric interferences (e.g. Kr, Rb, Ca dimers, etc.) as LA-ICP-MS techniques (e.g., Ramos et al., 2004; Vroon et al., 2008). By pairing the TIMS Sr isotopic data with Nd isotopic analyses and major, trace, and volatile element data on the same melt inclusions, this study provides new constraints on the origin of $^{87}Sr/^{86}Sr$ variability in olivine-hosted melt inclusions in oceanic hotspot lavas.

2. Methods

2.1. Sample selection

The samples—AVON3-71-2 from Vailulu'u seamount in Samoa (Jackson and Hart, 2006), and an olivine-rich scoria clast from the Pu'u Wahi eruption on Mauna Loa, Hawai'i (Sobolev et al., 2011; Wallace et al., 2015) (see Fig. 1)—were chosen for this study based on prior observations of $^{87}Sr/^{86}Sr$ heterogeneity within their olivine-hosted melt inclusion populations. Additionally, each of these samples contain abundant olivines that host abundant, large ($>$ 100 µm) melt inclusions.

2.1.1. Vailulu'u sample AVON3-71-2

This sample is a deeply dredged picrite from Vailulu'u (the active location of the Samoan hotspot) that has been extensively characterized geochemically, including whole-rock major- and trace-element concentrations, $^{87}Sr/^{86}Sr$, $^{143}Nd/^{144}Nd$, $^{208}Pb/^{204}Pb$, $^{207}Pb/^{204}Pb$, $^{206}Pb/^{204}Pb$, $^{176}Hf/^{177}Hf$, and $^{187}Os/^{188}Os$ (Workman et al., 2004; Salters et al., 2011; Jackson and Shirey, 2011). Additionally, major, trace, and volatile-element concentrations were measured in glass (Workman et al., 2006; Kendrick et al., 2015), $^{87}Sr/^{86}Sr$ was measured in individual melt inclusions using LA-MC-ICP-MS (Jackson and Hart, 2006), $\delta^{18}O$ and $^{3}He/^{4}He$ were reported in olivines (Workman et al., 2004, 2008), $^{87}Sr/^{86}Sr$ and $^{143}Nd/^{144}Nd$ isotopic ratios were measured in clinopyroxene separates (Jackson et al., 2009), and $^{87}Sr/^{86}Sr$ was measured on bulk olivine separates (Reinhard et al., 2016).

2.1.2. Pu'u Wahi

Pu'u Wahi is a line of scoria cones on the NE rift zone of Mauna Loa (Lockwood, 1995). Olivine-hosted melt inclusions in scoria have the advantage of having been rapidly cooled, resulting in glass melt inclusions. The material sampled is a reticulite scoria clast hosting abundant euhedral olivines (referred to hereafter as the “Pu'u Wahi” sample), and material from this eruption was analyzed for major, trace, and select volatile-element (S and Cl) concentrations, as well as $^{87}Sr/^{86}Sr$, $^{207}Pb/^{206}Pb$, and $^{208}Pb/^{206}Pb$ isotopic ratios in olivine-hosted melt inclusions (Sobolev et al., 2011). In the same study, major-element concentrations in the glass matrix and host olivines, trace-element concentrations, and $^{87}Sr/^{86}Sr$ in Pu'u Wahi matrix glass were reported. Olivines from Pu'u Wahi were also used for experimental testing of H diffusion rates in olivine by Gaetani et al. (2012), and a later study measured major element and volatile (H_2O, CO_2, S) concentrations in olivine-hosted melt inclusions from the Pu'u Wahi scoria (Wallace et al., 2015).

2.2. Sample preparation

Sample AVON3-71-2 was crushed using a rock hammer then sieved before olivines were handpicked under a binocular microscope. The Pu'u Wahi sample is glass rich, and adhering glass had to be removed from the olivines prior to sample preparation. Therefore, the Pu'u Wahi olivines, but not the AVON3-71-2 olivines, were leached in 2N HF for 10 min at 25 °C, then rinsed three times in milli-Q water, then leached in concentrated

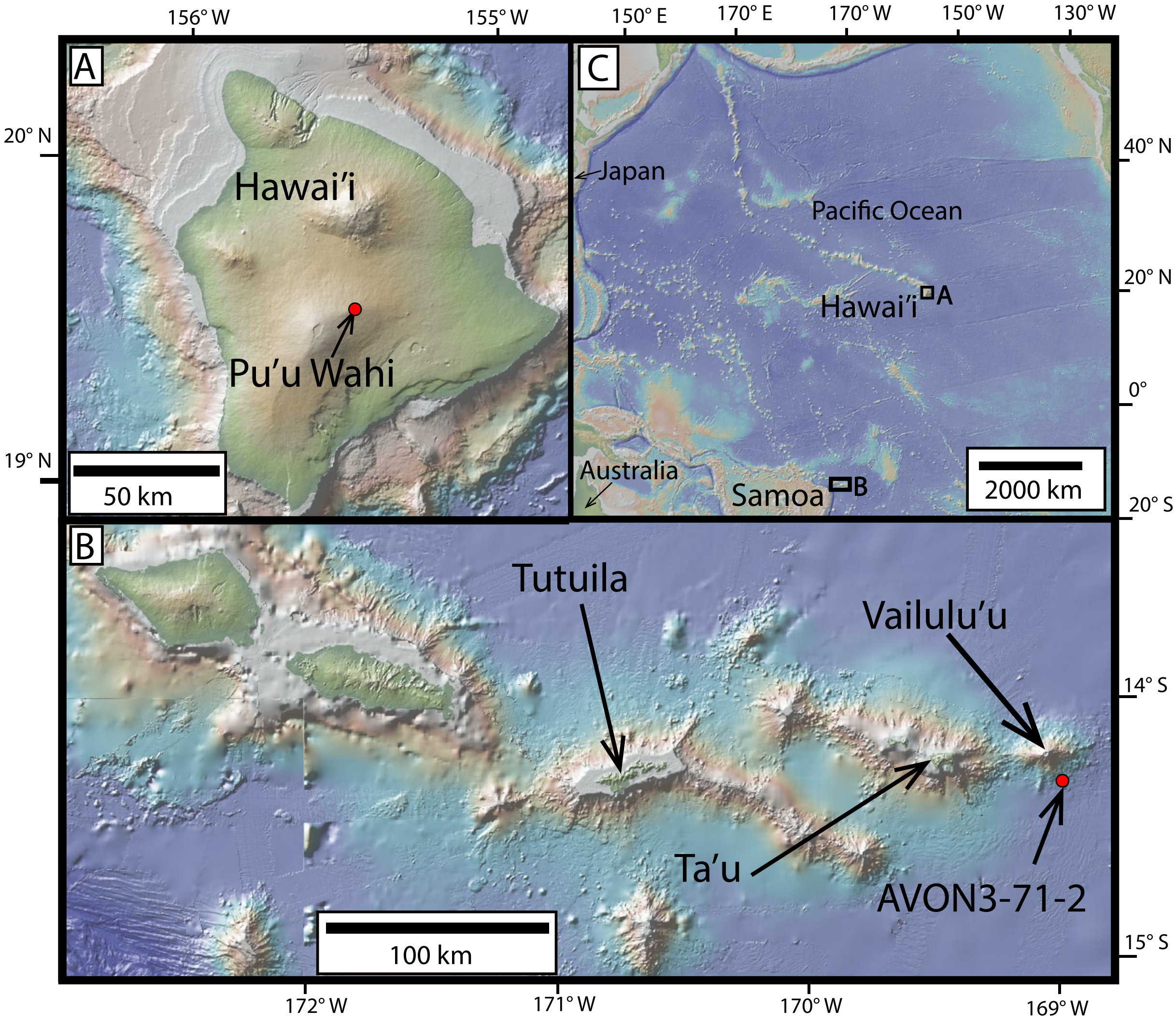

Fig. 1. Map of sample locations for A) the Hawai'ian Pu'u Wahi flow on Mauna Loa and B) the Samoan sample AVON3-71-2 from Vailulu'u seamount. Panel C shows the Pacific region and the relative location of each sample. The base map imagery is from GeoMapApp (geomapapp.org).

HNO_3 for 15 min at 25 °C, then rinsed again three times in milli-Q water to remove all adhering matrix glass. Visual inspection and geochemical analytes indicate that the process of leaching the adhering glass off of the olivine surfaces did not modify the entrapped Pu'u Wahi melt inclusions, which were protected within the olivine crystal. Olivines that hosted large (> 85 µm) melt inclusions were selected from both samples (AVON3-71-2, $N = 10$ melt inclusions; Pu'u Wahi, $N = 10$; Table 1 and Tables S1 to S7). The selected olivines hosting large melt inclusions were inspected under a binocular microscope to ensure that there was no remaining matrix glass, basaltic groundmass, or secondary phases. Because some olivines host more than one melt inclusion, some of the selected olivines hosting melt inclusions were then cut with a diamond wire saw (150 µm diameter wire) to isolate the largest melt inclusion; remaining melt inclusions hosted in the same olivine grain were removed by mounting the olivine in Crystalbond™ and grinding the melt inclusions with silicon carbide abrasive paper (See Fig. 2 for graphic of melt inclusion isolation). Most grains required polishing in multiple orientations to remove visible melt inclusions. Through this process, all visible glass, groundmass, and/or surface alteration was also removed from the olivines by making strategic cuts with the diamond wire saw and by grinding with silicon carbide (Fig. 2) (images of melt inclusions are shown in Fig. S1). The olivines were then removed from their mounts, sonicated in acetone for 15 min to remove any adhering Crystalbond ™, leached in 6 N HCl at 25 °C for 10 min, and then rinsed three times in milli-Q (i.e., 18.2 MΩ) water.

While the Pu'u Wahi melt inclusions were dominantly glassy (only 2 melt inclusions required homogenization), all inclusions from AVON3-71-2 were crystalline and necessitated homogenization. Following isolation of melt inclusions by cutting and polishing, olivine fragments hosting a single large melt inclusion were homogenized using a Vernadsky-type heating stage under a microscope at the Laboratoire Magmas et Volcans at the Université Clermont Auvergne in Clermont-Ferrand, France, following the procedure detailed by Le Voyer et al. (2008). Crystalline melt inclusions were bathed in helium during homogenization at 1 atm and the oxygen fugacity was kept between 10^{-10} and 10^{-9} atm. Temperatures of homogenization (where applicable) can be found in Table S1. Samples were quenched after homogenization to avoid recrystallization of the melt inclusions. Samples that burst or cracked during homogenization were discarded and are not considered in this study (note that three melt inclusions from AVON3-71-2 did not fully homogenize during heating on the Vernadsky-type stage, therefore we do not discuss their major or trace element concentrations, but we do present and discuss their Sr and Nd isotopic compositions). The resultant glassy melt inclusions were then exposed by careful grinding and polishing, pressed into an indium mount, re-polished using ¼ µm alumina paste, ultra-sonicated in ethanol (10 min) and then distilled water (10 min) before major and trace element analysis.

Unlike Harlou et al. (2009), who separated the melt inclusions from the host olivine by micro-drilling, this study does not separate melt

Table 1
Sr and Nd isotopic measurements made on melt inclusions in this study.

Sample[a]	Total Sr (ng)	Sample to blank ratio (Sr)	$^{87}Sr/^{86}Sr$[b]	2σ (std. err.)	Total Nd (ng)	Sample to blank ratio (Nd)	$^{143}Nd/^{144}Nd$[c]	2σ (std. err.)
Vailulu'u[d]								
AVON3-71-2-1	3.0	42	0.705221	0.000012	0.24	41	0.512809	0.000065
AVON3-71-2-2	4.3	59	0.705508	0.000023				
AVON3-71-2-3	1.8	25	0.705853	0.000036				
AVON3-71-2-5	4.8	66	0.705307	0.000011	0.40	66	0.512705	0.000052
AVON3-71-2-8	4.3	59	0.705229	0.000012	0.31	51	0.512745	0.000078
AVON3-71-2-9	2.7	37	0.705193	0.000016				
Puu Wahi[d]								
PW-1	2.0	28	0.703902	0.000011				
PW-2	2.0	28	0.703935	0.000030				
PW-3	2.9	40	0.703938	0.000018				
PW-4	7.4	103	0.703906	0.000012	0.38	63	0.512800	0.000050
PW-5	5.4	75	0.703871	0.000015	0.24	40	0.512900	0.000064
PW-8	4.1	57	0.703807	0.000040				
PW-9a	4.0	56	0.703903	0.000013				
PW-10	19.1	265	0.703777	0.000010	1.07	178	0.512876	0.000047
PW-11	3.4	47	0.703761	0.000011				

[a] Only Pu'u Wahi melt inclusions PW-5 and PW-9a were homogenized, and none of the other Pu'u Wahi melt inclusions were homogenized; all AVON3-71-2 melt inclusions were homogenized.

[b] $^{87}Sr/^{86}Sr$ values have been blank corrected and corrected for the offset between the preferred (0.710240) and the measured $^{87}Sr/^{86}Sr$ of NBS987.

[c] $^{143}Nd/^{144}Nd$ values have been blank corrected and corrected for the offset between the preferred (0.512104) and the measured $^{143}Nd/^{144}Nd$ of JNdi-1.

[d] Only inclusions with Sr_{sample}/Sr_{blank} ratios > 25 and Nd_{sample}/Nd_{blank} ratios > 40 are shown in the table. Inclusions with lower sample/blank ratios are not discussed in the text, but are included in Tables S7 and S8.

inclusions from the olivine. This is because Sr and Nd are highly incompatible in the olivine lattice (Fujimaki et al., 1984; Beattie, 1994) and therefore the Sr and Nd budgets of the olivines are dominated by the melt inclusions (Koornneef et al., 2015). It is not possible to avoid micro-inclusions during sample preparation, but their influence on the Sr (or Nd) isotopic composition of the target melt inclusion will be minimal. For example, the $^{87}Sr/^{86}Sr$ composition of a 150 µm diameter melt inclusion with $^{87}Sr/^{86}Sr$ of 0.7050 (and 300 ppm Sr) would be perturbed by only 0.2 ppm if a 5 µm diameter melt inclusion—which is visible under a binocular microscope—with $^{87}Sr/^{86}Sr$ of 0.7092 (and the same Sr concentration) was inadvertently included in the same olivine through sample preparation and digestion.

2.3. Major and trace element analyses

Major-element, Cl and S concentrations of the melt inclusions, and major element concentrations of the olivines, were carried out using the Cameca SX100 electron microprobe hosted at the Laboratoire Magmas et Volcans following the method described by Le Voyer et al. (2008). A focused electron beam with 15 kV accelerating voltage and 15 nA current was used for analyses of host olivines. For analyses of melt inclusions, an electron beam defocused to 5 µm with 15 kV accelerating voltage and 8 nA current was used. Analyses of ALV519-4-1 (Melson et al., 2002) and KL2-G (Jochum et al., 2006) were performed throughout the major element analytical session to monitor for instru-

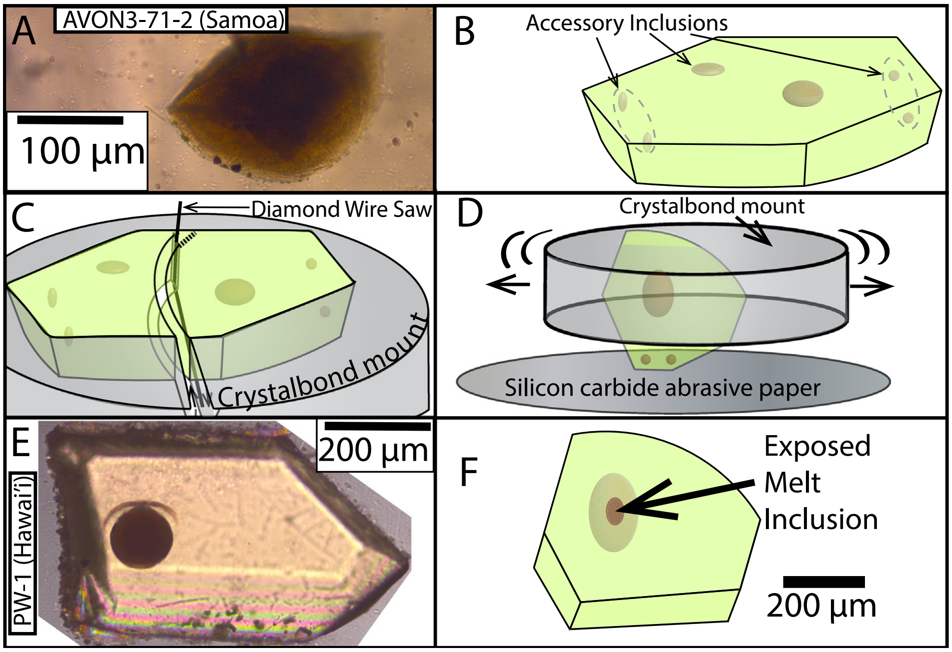

Fig. 2. Olivine preparation schematic. Panel A is a photograph of a homogenized melt inclusion (AVON3-71-2-6) analyzed in this study (images of all melt inclusions are shown in Fig. S1). Prior to Sr and Nd isotopic analyses of melt inclusions, olivines with accessory inclusions were identified and accessory inclusions were removed (B), using a diamond wire saw to cut away portions of the olivine that contain accessory inclusions (C), then polishing away any remaining accessory inclusions (D), and finally exposing a small portion of the melt inclusion by polishing for EPMA, SIMS, and LA-ICP-MS analyses (F). Panel E is an example of a melt inclusion (PW-1) that has been successfully isolated from accessory inclusions. Accessory inclusions include smaller melt inclusions, fluid inclusions, and spinel crystals.

ment drift and data quality, and several standards were analyzed during the Cl and S analytical session (including ALV519-4-1; see Table S2). Reproducibility for basaltic glass reference material ALV519-4-1 was < 2% (2 RSD) for SiO_2, Al_2O_3, MgO, and CaO, < 3% for TiO_2, ≤ 5% for FeO and Na_2O, < 23% for K_2O, < 39% for MnO, and < 68% for P_2O_5. Reproducibility is calculated based on repeat analyses of basaltic geologic reference glasses during the same analytical session. Chlorine and S were measured 5 times consecutively in each melt inclusion and standard using a 40 s cycle, and errors are based on the reproducibility of these consecutive analyses.

Data for melt inclusions, olivines, and geologic reference materials can be found in Tables S1, S2, S3, and S4. Major-element data were corrected for the effects of post-entrapment crystallization of olivine by adding (or subtracting) equilibrium olivine to the melt inclusions in 0.1% increments until the melt inclusion is in equilibrium with the host olivine. Calculation of equilibrium olivine assumes an olivine-melt Fe-Mg K_d of 0.30 ± 0.03 (Roeder and Emslie, 1970; Ford et al., 1983) and that 10% of the total iron in the melt is as Fe^{3+}. These olivine-corrected values are reported in Table S5. Unless stated otherwise, all melt inclusion major (and trace, see below) element compositions discussed in the text have been corrected for olivine addition (or fractionation).

Trace element concentrations were measured using a Thermo Scientific Element XR ICP-MS coupled to a Resonetics M-50E 193 nm ArF excimer laser housed at Laboratoire Magmas et Volcans. The method followed those outlined in Oulton et al. (2016), with some minor differences as described here. Intensities were normalized to ^{43}Ca as the internal standard. Before all analyses, each spot underwent preablation for 1 s at 10 Hz repetition rate to remove surface contamination. Analyses of melt inclusions and geologic reference materials used a 20 μm spot and had a repetition rate of 2 Hz with a 50 s dwell time (resulting in 100 shots per spot); the laser pits were approximately 15 μm deep. The accelerating voltage was scanned between magnet jumps to monitor the peak positions. The following masses were analyzed for the target elements ^{6}Li, ^{7}Li, ^{44}Ca, ^{47}Ti, ^{59}Co, ^{85}Rb, ^{88}Sr, ^{89}Y, ^{90}Zr, ^{93}Nb, ^{137}Ba, ^{139}La, ^{140}Ce, ^{146}Nd, ^{147}Sm, ^{157}Gd, ^{172}Yb, ^{208}Pb, ^{238}U. Analyses were made in low resolution mode using triple mode with a 20% mass window and a 20 ms integration window. NIST612 (Gagnon et al., 2008) and BCR-2 (Jochum et al., 2006) glass were used as standards to generate the calibration curve. Trace element concentrations are shown in Table S3, and olivine-fractionation corrected trace element concentrations of the melt inclusions are shown in Table S6 (for the olivine-fractionation correction, incompatible trace element concentrations were adjusted by the same proportion as incompatible major elements, e.g., TiO_2). To evaluate the precision and accuracy of analyses, 16 replicate trace element measurements were performed on a basaltic glass sample GL07-D52-5 (an incompatible trace element enriched glass from the Easter-Salas y Gomez seamount chain from Kelley et al., 2013), with trace element concentrations similar to those in the Hawai'ian melt inclusions from Pu'u Wahi, but somewhat more depleted than the incompatible trace element enriched Samoan melt inclusions from Vailulu'u. The reproducibility of the trace element concentrations measured in this basaltic glass reference material (see Table S2) was better than 6% (2 RSD, $N = 16$), except for Pb (8%), and U and Li (10% and 12%, respectively). The measured concentrations agree with published values from Kelley et al. (2013) to better than 6% for most elements (Ti, Sr, Nb, Ba, La, Ce, Nd, Sm, Yb), and better than 10% for the remaining elements (see Table S2). We report volatile elements (CO_2, H_2O, and F) in the supplementary tables. Methods can be found in the supplementary material.

2.4. $^{87}Sr/^{86}Sr$ and $^{143}Nd/^{144}Nd$ analysis of melt inclusions by TIMS

Olivines were plucked from the indium mount and then leached in 15 N nitric acid for 2 min at 90 °C to remove any adhering indium. Samples were then leached in 1 N HCl for 15 min at 25 °C to remove any remaining surface contamination and transferred to Teflon beakers. Spikes of ^{84}Sr and ^{150}Nd were added to each olivine sample, for determination of the total amount of analyte in the sample. The olivines (and the melt inclusions hosted within) were then dissolved in a 4:1 solution of concentrated HF and concentrated HNO_3, and placed on a hot plate at 120 °C in capped Teflon beakers for 4 days. Samples were then dried down and brought up in concentrated HNO_3. Finally, samples were brought up in 200 μl of 3 N HNO_3 and loaded on to columns for chemical separation of Sr and Nd. Chemical separation followed the procedures detailed in Koornneef et al. (2015).

The separated Sr was then loaded onto degassed Re filaments for $^{87}Sr/^{86}Sr$ analyses on the Thermo Scientific Triton *Plus* TIMS housed at the Vrije Universiteit (VU) Amsterdam. Strontium isotopic and abundance measurements were made using ID-TIMS with standard $10^{11}\,\Omega$ amplifiers and a static multi-collection routine (Koornneef et al., 2015). All $^{87}Sr/^{86}Sr$ ratios were corrected for mass bias relative to an accepted $^{86}Sr/^{88}Sr$ ratio of 0.1194 using an exponential law. Two 200 ng loads of NBS987 were analyzed during the same analytical session and had $^{87}Sr/^{86}Sr$ ratios of 0.710236 (± 0.000009, 2 SE) and 0.710243 (± 0.000009, 2 SE). All $^{87}Sr/^{86}Sr$ ratios measured on melt inclusions and geologic reference materials are corrected for the offset between the preferred NBS987 value (0.710240; Thirlwall, 1991) and the average value measured on NBS987 during the same analytical session. Two aliquots of BHVO-2 (146 and 380 ng of Sr) were processed through all steps of the chemistry, and yielded $^{87}Sr/^{86}Sr$ ratios of 0.703470 (± 0.000010, 2 SE) and 0.703458 (± 0.000008, 2 SE). Both measured BHVO-2 compositions are within error of the preferred BHVO-2 value of 0.703471 (± 0.000020, 2 SD), following renormalization to a NBS987 value of 0.710240 (Weis et al., 2006). The average $^{87}Sr/^{86}Sr$ of AGV-1 (loaded to have ~4 ng Sr) run during the same period was 0.704007 (± 0.000029 2 SD, $N = 6$), which is within error of the preferred AGV-1 value of 0.703981 (± 0.000017 2 SD; Weis et al., 2006), following renormalization to the preferred NBS987 value of 0.710240.

Neodymium was loaded onto a degassed Re filament for $^{143}Nd/^{144}Nd$ ratio and Nd abundance analyses on the Thermo Scientific Triton *Plus* using $10^{13}\,\Omega$ amplifiers in the feedback loop (following procedures from Koornneef et al., 2014, 2015). The $10^{13}\,\Omega$ amplifiers yield better signal-to-noise ratios that enhance the precision of isotopic analyses of very small amounts of Nd (Koornneef et al., 2014, 2015). All $^{143}Nd/^{144}Nd$ ratios were corrected for instrumental mass bias to a $^{146}Nd/^{144}Nd$ ratio of 0.7219 using the exponential law. All $^{143}Nd/^{144}Nd$ ratios are corrected for the offset between the measured JNdi value (measured during the same analytical session) and our preferred value (0.512104; Hamelin et al., 2011). Three 100 ng JNdi standards were run throughout the analytical session using $10^{13}\,\Omega$ amplifiers, and yielded values of 0.512111 (± 0.000032, 2 SE), 0.512154 (± 0.000035, 2 SE) and 0.512116 (± 0.000035 2 SE); the average $^{143}Nd/^{144}Nd$ value was used to correct for the offset of the measured value from the preferred value. Additionally, a 100 pg load of the in-house CIGO standard was run, yielding a $^{143}Nd/^{144}Nd$ value of 0.511357 (± 0.000034, 2 SE), which is within error of the long-term average of 100 pg CIGO standard loads run at VU using the same technique (0.511339 ± 0.000066 2 SD, $N = 77$). Two (9.3 and 23 ng Nd) aliquots of BHVO-2 were processed through all steps of the Nd chemistry with the melt inclusions in this study, and yielded $^{143}Nd/^{144}Nd$ ratios of 0.512969 (± 0.000039, 2 SE) and 0.512908 (± 0.000037, 2 SE); these values compare well with the Weis et al. (2006) BHVO-2 value of 0.512973 (± 0.000011 2 SD), following the La Jolla to JNdi conversion from Tanaka et al. (2000) and correcting to a JNdi $^{143}Nd/^{144}Nd$ value of 0.512104. The average $^{143}Nd/^{144}Nd$ of AGV-1 (loaded to have ~200 pg Nd) run during the same period was 0.512793 (± 0.000040, 2 SD, $N = 4$; normalized to a CIGO value of 0.511339), which is within error of the preferred Weis et al. (2006) AGV-1 value of 0.512780 (± 0.000013, 2 SD) following the corrections used above.

Individual Samoan and Hawai'ian melt inclusions contained 0.8 to 19.1 ng of Sr (Table 1 & S7) and 0.06 to 1.07 ng of Nd (Table 1 & S8). Total procedural blanks were processed together with the melt inclusions through all steps of column chemistry and mass spectrometry and were 72 pg for Sr

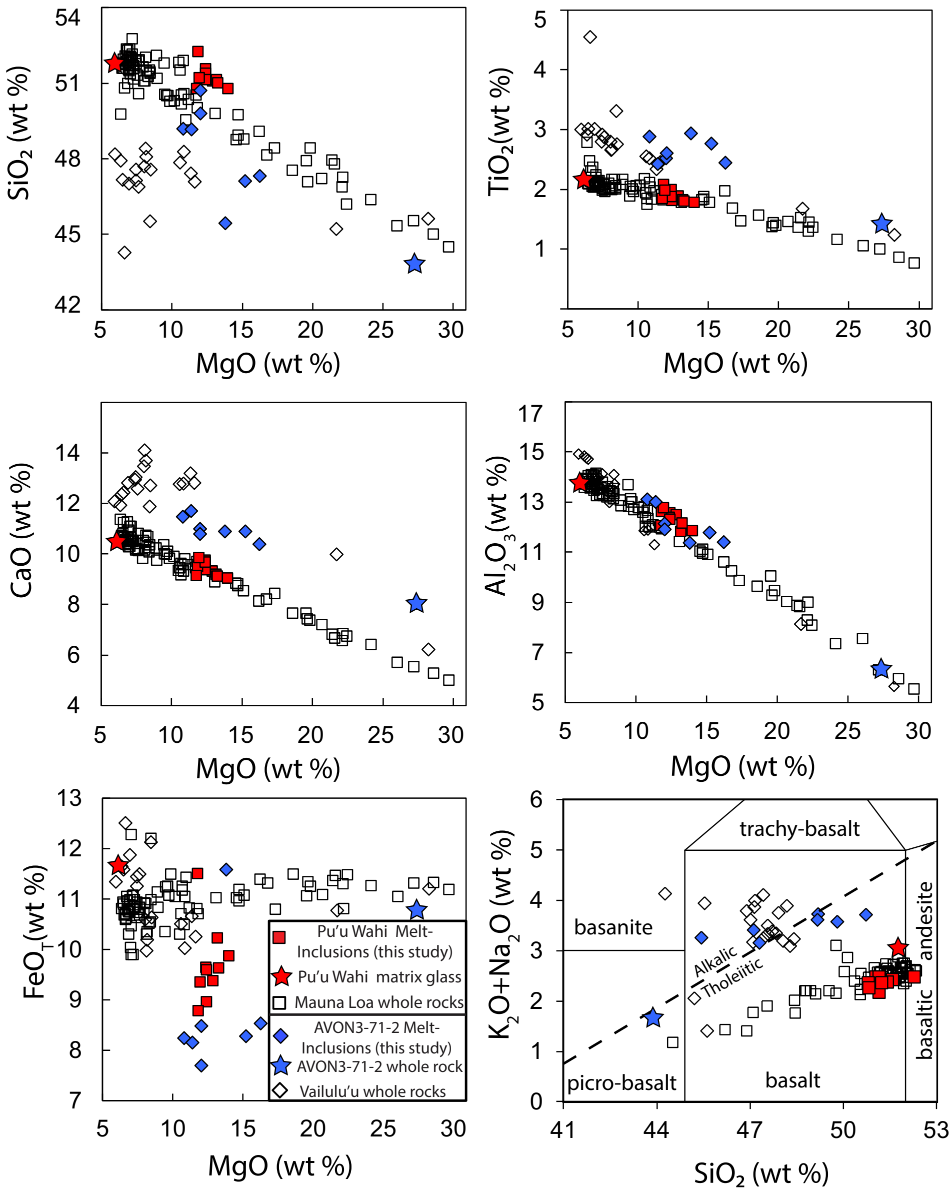

Fig. 3. Major-element compositions of the Pu'u Wahi and AVON3-71-2 melt inclusions. Vailulu'u whole rock data are from Workman et al. (2004) and Jackson et al. (2010). Mauna Loa whole rock data were taken from the GeoRoc [http://georoc.mpch-mainz.gwdg.de] compilation of Hawai'ian lavas, and only lavas with > 6 wt% MgO are shown. Melt inclusion major elements are corrected for olivine crystallization to be in equilibrium with the host olivine and are normalized to 100 wt% totals (on a dry basis).

and 6 pg for Nd. Sample-to-blank ratios for Sr analyses varied from 11 to 265, and from 10 to 178 for Nd (see Tables S7 & S8). A sample-to-blank threshold was applied to ensure that samples with the most significant contribution from blank were not considered, and the following thresholds are employed to reduce uncertainty associated with the blank correction (see Fig. S2): Only analyses with Sr sample/blank ratios > 25, and Nd sample/blank ratios > 40, are considered in Sections 3 (Data and Observations) and Section 4 (Discussion). Nonetheless, all Sr and Nd isotopic data, including melt inclusions that have unacceptably low sample/blank ratios, are reported in Tables S7 and S8. Blank corrections were made using the laboratory blank $^{87}Sr/^{86}Sr$ and $^{143}Nd/^{144}Nd$ ratios previously determined for the Sr and Nd chemistry at VU (Koornneef et al., 2015; Knaf et al., 2017); the total procedural blank isotopic ratio used for correction is 0.711120 ± 0.000050 ($N = 3$) for $^{87}Sr/^{86}Sr$ and 0.511856 ± 0.000090 ($N = 3$) for $^{143}Nd/^{144}Nd$.

3. Data and observations

Major elements for the melt inclusions analyzed in this study are presented in Fig. 3 (and Table S1 & S5). Like all Mauna Loa lavas, the 10 olivine-hosted melt inclusions analyzed in this study are tholeiitic, whereas three melt inclusions from AVON3-71-2 are alkalic and four are transitional (Fig. 3). The MgO contents of the Pu'u Wahi (11.8–14.1 wt%; Table S5) and AVON3-71-2 (10.9–16.3 wt%; Table S5) melt inclusions fall within the range identified in previously analyzed Mauna Loa and Vailulu'u lavas, respectively (Fig. 3). With the exception of one Pu'u Wahi and one AVON3-71-2 melt inclusion, the melt inclusions from both samples have significantly lower FeO concentrations than previously analyzed Mauna Loa and Vailulu'u whole rocks (Fig. 3). The apparent depletion in Fe in most of the melt inclusions, due to re-equilibration between the melt inclusion and the host olivine, is similar to previous observations of "Fe-loss" from olivine-hosted melt

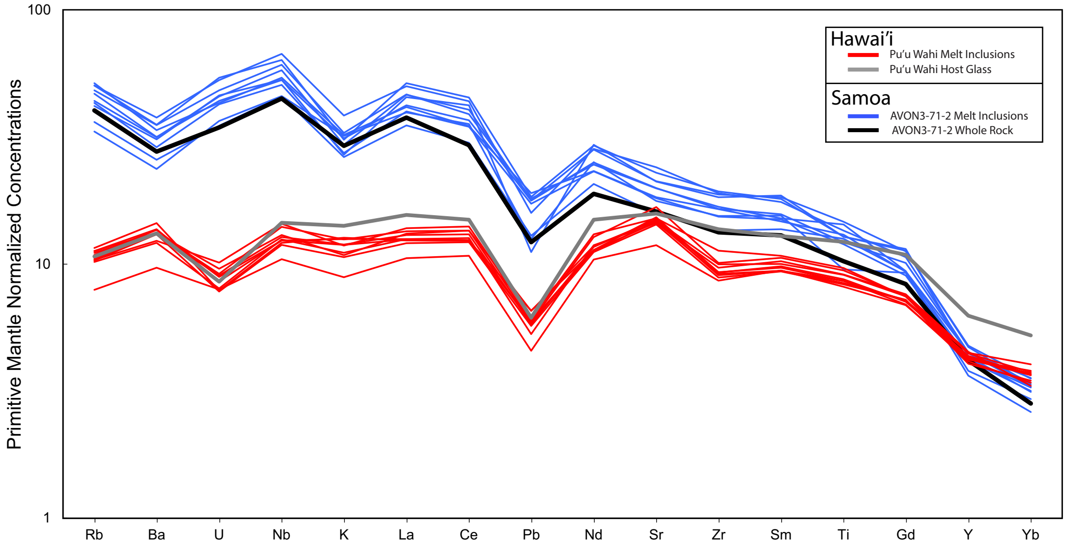

Fig. 4. Primitive mantle–normalized trace-element patterns from the seven glassy AVON3-71-2 melt inclusions and ten glassy Pu'u Wahi melt inclusions presented in this study (normalized to the primitive mantle values from McDonough and Sun, 1995). The black line is the trace-element data for the AVON3-71-2 whole rock from Workman et al. (2004), corrected for olivine accumulation (or fractionation) to be in equilibrium with Fo_{90}. The grey line is the trace-element data for the host glass for the Pu'u Wahi olivines (Sobolev et al., 2011).

inclusions at other localities (Danyushevsky et al., 1992, 2000; Sobolev and Danyushevsky, 1994; Gaetani and Watson, 2000; Kent, 2008).

Following correction for olivine addition (or fractionation) to be in equilibrium with the host olivine, the primitive mantle (McDonough and Sun, 1995) normalized incompatible trace element patterns of the melt inclusions from AVON3-71-2 are similar to that of the host whole rock (Fig. 4). The AVON3-71-2 melt inclusions have no clear Sr anomalies relative to elements of similar compatibility. (Sr anomalies are represented by $Sr/Sr^* = Sr_N/(Nd_N * Sm_N)^{0.5}$, where N represents normalization to the primitive mantle concentration from McDonough and Sun (1995)). In the Pu'u Wahi melt inclusions, trace element concentrations of the most incompatible elements are similar to their host glass. In contrast, the less incompatible elements (Zr, Sm, Ti, Gd, Y, Tb) tend to have lower concentrations in the melt inclusions relative to host glass analyzed by Sobolev et al. (2011), but we do not have an explanation for this observation. The Pu'u Wahi melt inclusions show positive Sr anomalies (average $Sr/Sr^* = 1.37$) that are generally larger in magnitude than the host glass ($Sr/Sr^* = 1.14$; Fig. 4).

Fig. 5a presents previously-published $^{87}Sr/^{86}Sr$ data obtained on various components of the Samoan lava AVON3-71-2 for comparison with the new $^{87}Sr/^{86}Sr$ reported on melt inclusions here, which are isotopically heterogeneous. Bulk whole rock $^{87}Sr/^{86}Sr$ (0.705943; Workman et al., 2004), LA-MC-ICP-MS data from melt inclusions (which were previously found to vary from 0.70459 to 0.70602; Jackson and Hart, 2006), bulk clinopyroxene separates (divided into two sub-populations based upon color: green [0.705485] and black [0.705545] cpx; Jackson et al., 2009), and aggregated olivine separates (also sub-divided based upon olivine color: green [0.705404] and brown [0.705436] olivine; Reinhard et al., 2016) are presented. The new $^{87}Sr/^{86}Sr$ data on individual olivine-hosted melt inclusions analyzed by TIMS in this study have $^{87}Sr/^{86}Sr$ values that range from 0.705193–0.705853 (936 ppm variability), which represents 44% of the total variability observed in previously analyzed *whole rocks* from Vailulu'u seamount. The $^{87}Sr/^{86}Sr$ measured in AVON3-71-2 melt inclusions in this study are consistent with previously observed values obtained on a separate suite of *melt inclusions* analyzed by Jackson and Hart (2006) using LA-MC-ICP-MS, but the new data (0.705193–0.705853; $N = 6$) span only 46% of the range of $^{87}Sr/^{86}Sr$ values identified in the LA-MC-ICP-MS data (0.70459 to 0.70602; $N = 12$). All melt inclusions from AVON3-71-2 in this study (by TIMS) and in a prior study (by LA-MC-ICP-MS), as well as all clinopyroxene separates and bulk aggregate olivines from this lava, have $^{87}Sr/^{86}Sr$ that is similar to or lower than the whole-rock (0.705943; Workman et al., 2004).

All published $^{87}Sr/^{86}Sr$ data from the Pu'u Wahi sample are presented in Fig. 5b, including data on the host glass (this study), $^{87}Sr/^{86}Sr$ on 137 melt inclusions by single-collector LA-ICP-MS (Sobolev et al., 2011), and new $^{87}Sr/^{86}Sr$ data in melt inclusions by TIMS reported here. Sobolev et al. (2011) found extreme $^{87}Sr/^{86}Sr$ variability (~8500 ppm) in a suite of melt inclusions from Pu'u Wahi (0.7021–0.7081; $N = 137$). In contrast, the Pu'u Wahi melt inclusions analyzed in this study show only 251 ppm of total variability (0.703761–0.703938, $N = 9$), which is > 30 times less variability than observed by Sobolev et al. (2011). Additionally, the Pu'u Wahi melt inclusions analyzed in this study have $^{87}Sr/^{86}Sr$ ratios that are less than, or within error of, the $^{87}Sr/^{86}Sr$ of the matrix glass (0.703912 ± 0.000008, 2 SE; this study) hosting the olivines. This stands in contrast to the Pu'u Wahi melt inclusions analyzed by Sobolev et al. (2011), which have $^{87}Sr/^{86}Sr$ ratios that are higher (64 melt inclusions) and lower (73 melt inclusions) than the matrix glass.

No $^{143}Nd/^{144}Nd$ heterogeneity outside of error was found in the Pu'u Wahi or AVON3-71-2 melt inclusions. Fig. 6 presents the $^{143}Nd/^{144}Nd$ and $^{87}Sr/^{86}Sr$ data of the Samoan and Hawai'ian melt inclusions analyzed in this study (see Table 1). Vailulu'u sample AVON3-71-2 melt inclusions with Nd-isotopic data ($N = 3$) have $^{143}Nd/^{144}Nd$ ratios of 0.512705 (± 0.000052, 2SE) to 0.512809 (± 0.000065, 2 SE), and are thus within error of previously reported whole rock $^{143}Nd/^{144}Nd$ measurements from Vailulu'u from Workman et al. (2004). Similarly, the three Pu'u Wahi melt inclusions with $^{143}Nd/^{144}Nd$ data have ratios that are within error of one another (from 0.512800 ± 0.000050 to 0.512900 ± 0.000064) and within error of previously published $^{143}Nd/^{144}Nd$ from Mauna Loa whole rocks.

Notably, Fig. 6 shows that the internal errors obtained on individual melt inclusions from Samoa AVON3-71-2 (the 2σ standard errors range from 102 to 152 ppm, $N = 3$) and Pu'u Wahi (91 to 126 ppm, $N = 3$) are similar to the errors obtained using an older generation TIMS instrument on $^{143}Nd/^{144}Nd$ analyses of MORB and OIB whole rocks by DePaolo and Wasserburg (1976) (60 to 90 ppm, $N = 3$). Nonetheless, the precision (91 to 152 ppm, 2 RSE) on $^{143}Nd/^{144}Nd$ analyses of individual melt inclusions is insufficient to resolve any intra-lava heterogeneity in this sample suite. However, this may be due to the

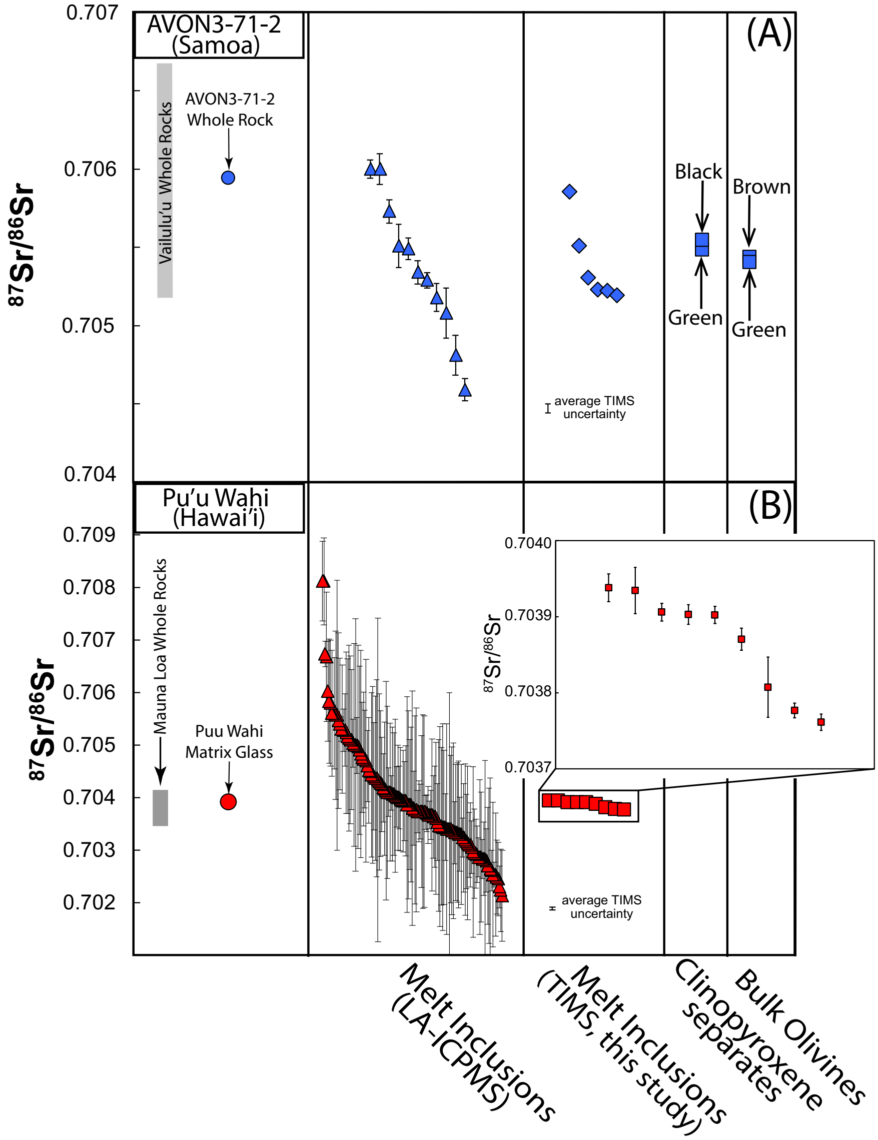

Fig. 5. All ^{87}Sr/^{86}Sr data published for AVON3-71-2 and Pu'u Wahi. In panel (A) ^{87}Sr/^{86}Sr data are presented for the AVON3-71-2 whole rock (Workman et al., 2004), melt inclusions by LA-MC-ICP-MS (Jackson and Hart, 2006), melt inclusions by TIMS (this study), clinopyroxene separates (separated by color; Jackson et al., 2009), and aggregated olivine (separated by color; Reinhard et al., 2016). The grey bar in (A) displays the total range of ^{87}Sr/^{86}Sr reported for Vailulu'u whole rocks by Workman et al. (2004), Jackson et al. (2010), and Jackson et al. (2014). For Pu'u Wahi, ^{87}Sr/^{86}Sr data for MC-ICP-MS host glass (this study), single-collector LA-ICP-MS melt inclusion (Sobolev et al., 2011), and TIMS melt inclusion (this study) are also presented in panel (B). For the LA-ICP-MS analyses of melt inclusions error bars are 2 SE, for all other data the error bars are smaller than the symbols. The grey bar in (B) displays the total ^{87}Sr/^{86}Sr variability reported in Mauna Loa whole rocks (compiled from the GEOROC database [http://georoc.mpch-mainz.gwdg.de]). The Pu'u Wahi host glass was analyzed as part of this study for ^{87}Sr/^{86}Sr (0.703912 ± 0.000008) and ^{143}Nd/^{144}Nd (0.512843 ± 0.000006) using the methods described in Hart and Blusztajn (2006), and the Sr and Nd isotopic data are normalized to the preferred NBS 987 (^{87}Sr/^{86}Sr = 0.710240) and JNdi (^{143}Nd/^{144}Nd = 0.512104) ratios.

geochemical nature of the melt inclusions that yielded successful ^{143}Nd/^{144}Nd analyses. For example, the three AVON-3-71-2 Samoan melt inclusions with ^{143}Nd/^{144}Nd measurements capture a relatively small fraction (0.705221 to 0.705307) of the total ^{87}Sr/^{86}Sr variability (0.705193 to 0.705853) present in melt inclusions from this lava. One might expect that, if the melt inclusions with the highest ^{87}Sr/^{86}Sr were to yield successful ^{143}Nd/^{144}Nd measurements, resolvable Nd-isotopic heterogeneity would also be observed. Future work will target these geochemically-enriched melt inclusions.

The ratio of chlorine to similarly incompatible elements (e.g. Nb) has been used as an indicator of assimilation of seawater derived materials or seawater-altered rocks in lavas (e.g. Rowe and Lassiter, 2009; Rose-Koga et al., 2012; Cabral et al., 2014). The Cl/Nb ratios vary from 13.4 to 16.6 in AVON3-71-2 melt inclusions, with the exception of melt inclusion AVON3-71-2-8 (33.6) (Fig. 7; Table S6). Similarly, high Cl/Nb ratios (up to 33.0 see Fig. 7) were observed in pillow rim glasses dredged from the flanks of Vailulu'u (Workman et al., 2006; Kendrick et al., 2015). In contrast, the Pu'u Wahi melt inclusions have Cl/Nb ratios (4.5–10.1) that are within the range suggested for mantle melts (Cl/Nb < 11; Rose-Koga et al., 2012). Cl/Nb (and Cl/K) do not co-vary with ^{87}Sr/^{86}Sr in the Pu'u Wahi or AVON3-71-2 melt inclusions analyzed in this study (Fig. 7).

However, ^{87}Sr/^{86}Sr ratios show a positive relationship with Rb/Sr and Ba/Nb ratios in AVON3-71-2 melt inclusions. The melt inclusions from AVON3-71-2 have Ba/Nb ratios that vary from 5.5 to 6.2, falling within the range of Ba/Nb previously reported on whole rock lavas from Vailulu'u (Fig. 8). The AVON3-71-2 melt inclusions have a smaller range in Rb/Sr (0.060–0.085) than previously observed in Vailulu'u lavas (0.051–0.081; Workman et al., 2004) (Fig. 9), but they fall within the range of Rb/Sr ratios (0.047–0.103) reported by Jackson and Hart (2006) in melt inclusions from the same sample (AVON3-71-2).

The Pu'u Wahi melt inclusions have a broad range of Ba/Nb ratios (8.6–12.0) that fall within the variability observed in Mauna Loa lavas (see Fig. 8). However, Sobolev et al. (2011) reported greater variability in Ba/Nb ratios of Pu'u Wahi melt inclusions (7.7–15.4) than we report in melt inclusions from the same lava. Similarly, Rb/Sr ratios in the Pu'u Wahi melt inclusions analyzed in this study (0.019–0.023; Fig. 9) exhibit an order of magnitude less variability than the Rb/Sr ratios observed in melt inclusions analyzed (0.004–0.045) by Sobolev et al. (2011). Finally, Sr isotopes in melt inclusions do not correlate with Rb/Sr in the new Pu'u Wahi melt inclusion dataset or in the dataset of Sobolev et al. (2011). However, in the Pu'u Wahi melt inclusions from this study there is a positive relationship between ^{87}Sr/^{86}Sr and Ba/Nb (Fig. 8), but no equivalent correlation is present in the Sobolev et al. (2011) dataset.

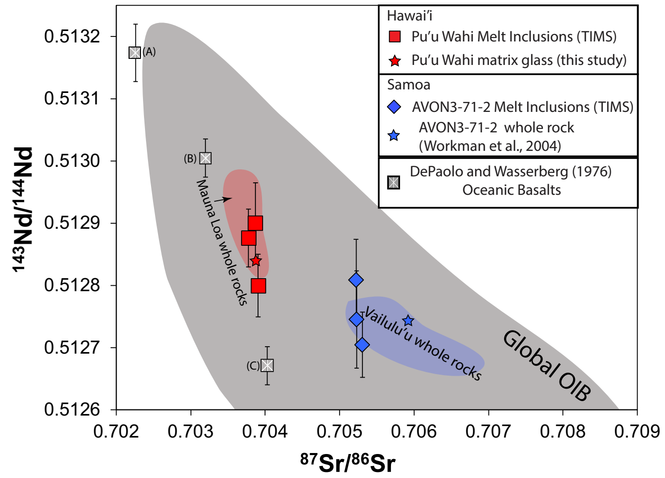

Fig. 6. $^{143}Nd/^{144}Nd$ versus $^{87}Sr/^{86}Sr$ for melt inclusions from Pu'u Wahi and AVON3-71-2. The grey field represents the global OIB array (compiled from the GEOROC database [http://georoc.mpch-mainz.gwdg.de]). Vailulu'u whole rock $^{87}Sr/^{86}Sr$ and $^{143}Nd/^{144}Nd$ data are from Workman et al. (2004), Jackson et al. (2010), and Jackson et al. (2014). Mauna Loa whole rock $^{87}Sr/^{86}Sr$ and $^{143}Nd/^{144}Nd$ data were compiled from the GEOROC database [http://georoc.mpch-mainz.gwdg.de]. Grey squares with white stars are $^{143}Nd/^{144}Nd$ analyses on oceanic basalts from DePaolo and Wasserburg (1976; A is Mid-Atlantic Ridge MORB [VG295], B is Oahu nephelinite [HN-1], C is Oahu tholeiite [HT-1]), and the precision from these early whole rock $^{143}Nd/^{144}Nd$ analyses is similar to the precision obtained on individual melt inclusions in this study. All error bars are 2 SE. Melt inclusions with low Sr and Nd sample/blank ratios are not plotted (see Methods and Fig. S2).

4. Discussion

4.1. Exploring mechanisms for generating $^{87}Sr/^{86}Sr$ variability in melt inclusions

Significant $^{87}Sr/^{86}Sr$ heterogeneity has been shown to exist between olivine-hosted melt inclusions within a single lava (Jackson and Hart, 2006; Harlou et al., 2009; Sobolev et al., 2011; Koornneef et al., 2015; this study). The observation that olivines in a single lava can host melts with variable $^{87}Sr/^{86}Sr$ necessitates that melts with variable $^{87}Sr/^{86}Sr$ were present when olivine crystallized in the magma system, and that olivines captured these heterogeneous melts as melt inclusions. Below, we discuss potential mechanisms for generating the heterogeneous melts trapped in the AVON3-71-2 and Pu'u Wahi melt inclusions: 1.) mixing of mantle-derived melts with variable $^{87}Sr/^{86}Sr$, and 2.) interaction with seawater-derived brines or interaction with material that has been significantly altered by seawater derived brine (hereafter referred to as "interaction with brines"). In the supplementary material we discuss 3.) assimilation of altered oceanic crust (AOC), and 4.) assimilation of unaltered gabbro in the deep oceanic crust, but we do not find evidence for these processes having modified the melt inclusions in this study. After acquiring heterogeneous $^{87}Sr/^{86}Sr$ and becoming entrapped in olivine, the olivine-hosted melt inclusion populations are assembled within magmatic plumbing systems and erupted.

Previous studies (Koornneef et al., 2015; Reinhard et al., 2016) argue that olivines encapsulate melts and preserve their $^{87}Sr/^{86}Sr$ ratios due to the incompatibility of Sr in olivine (Beattie, 1994) and slow Sr diffusion rates through olivine (Remmert et al., 2008). Additionally, both of the samples we studied have relatively low Rb/Sr ratios (see Data and Observations section) and are visually fresh and young—Pu'u Wahi erupted at 910 yr B.P. (Lockwood, 1995) and AVON3-71-2 is $<$ 8 ka (Sims et al., 2008)—such that the radiogenic decay of ^{87}Rb to ^{87}Sr (half-life of ~49 Ga) has not significantly modified the $^{87}Sr/^{86}Sr$ of these melt inclusions post entrapment. Therefore, we assume all $^{87}Sr/^{86}Sr$ heterogeneity in the melt inclusions examined here is the result of pre-entrapment processes. In the following sections we evaluate potential mechanisms that contribute to heterogeneous $^{87}Sr/^{86}Sr$ in melt inclusions: new data from Vailulu'u melt inclusions are explored, followed by a discussion of the relatively isotopically homogeneous Pu'u Wahi melt inclusions.

4.2. Vailulu'u (Samoan sample AVON3-71-2)

4.2.1. Mixing of mantle-derived melts with heterogeneous $^{87}Sr/^{86}Sr$

The mixing of mantle melts with heterogeneous $^{87}Sr/^{86}Sr$ has been proposed as a mechanism for generating the highly heterogeneous $^{87}Sr/^{86}Sr$ ratios in olivine-hosted melt inclusions, including melt inclusions from AVON3-71-2 (Jackson and Hart, 2006). If mantle melts have heterogeneous $^{87}Sr/^{86}Sr$ ratios that reflect their source, then the mixing of these melts as olivine is crystallizing (and trapping melt inclusions) could generate the observed $^{87}Sr/^{86}Sr$ and trace element ratio heterogeneity in the AVON3-71-2 melt inclusions.

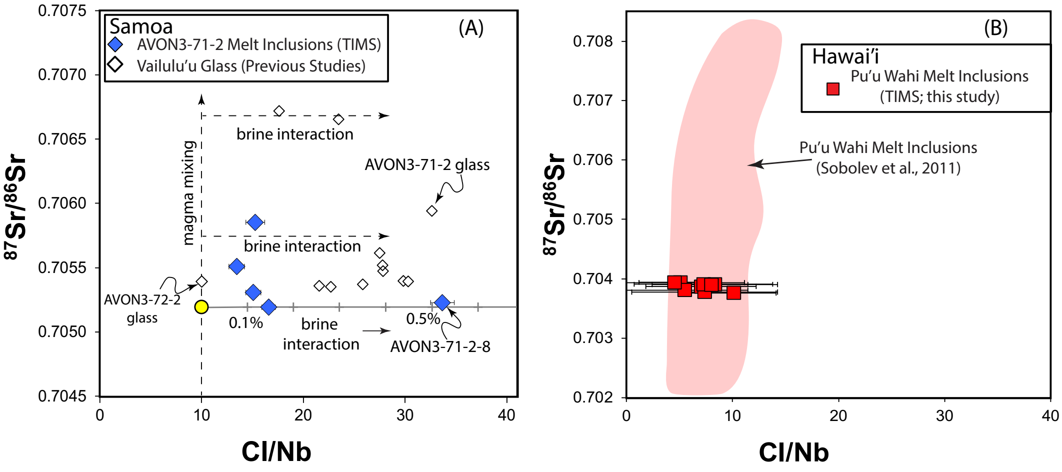

Fig. 7. Cl/Nb plotted versus $^{87}Sr/^{86}Sr$ for AVON3-71-2 (A) and Pu'u Wahi (B). Vailulu'u glass $^{87}Sr/^{86}Sr$ and Cl/Nb data in (A) are from Workman et al. (2006) and Kendrick et al. (2015). Where a glass from Workman et al. (2004) was reanalyzed by the noble gas method for Cl by Kendrick et al. (2015), the Kendrick et al. (2015) value for Cl is used. The grey line with grey tick marks is a binary mixing model of a model melt (yellow circle; described in Section 4.2.2) with a 55 wt% brine (as discussed in Section 4.2.2). Each tick mark represents 0.1% brine interaction. The vertical dashed line shows the effect of mixing the least contaminated (by seawater-derived materials) Vailulu'u melts and the horizontal dashed lines show the effect of interaction with brine. In (B) previously published Pu'u Wahi melt inclusion $^{87}Sr/^{86}Sr$ and Cl/Nb data from Sobolev et al. (2011) are represented by the red field. (For interpretation of the references to color in this figure legend, the reader is referred to the web version of this article.)

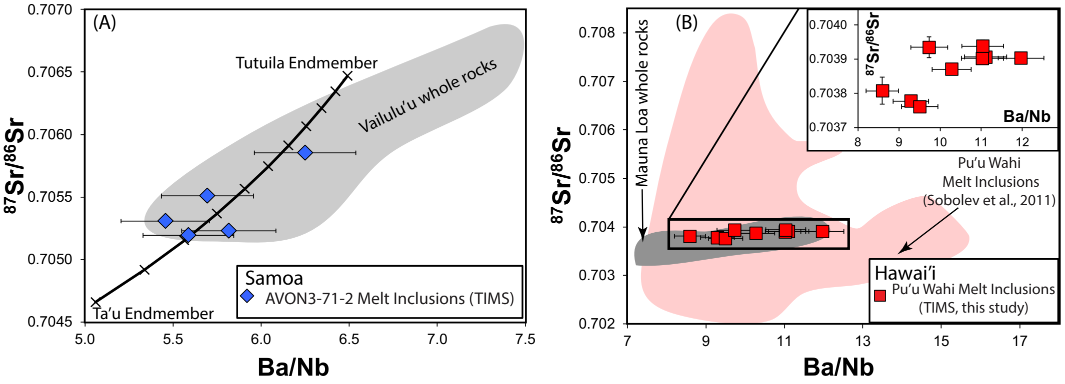

Fig. 8. ^{87}Sr/^{86}Sr versus Ba/Nb in the melt inclusions from AVON3-71-2 (A) and Pu'u Wahi (B). Vailulu'u whole rock ^{87}Sr/^{86}Sr and Ba/Nb field encompasses data from Workman et al. (2004), Jackson et al. (2010), and Jackson et al. (2014). The black line is a mixing model between Ta'u lava T10 (from Workman et al., 2004 [0.704657; 437 ppm Sr, 19.9 ppm Rb, 178 ppm Ba, and 35.2 ppm Nb]) and Tutuila Island basalt sample TGH3-1931. TGH3-1931 (the enriched mixing endmember in the mixing model) was analyzed for trace elements and ^{87}Sr/^{86}Sr using the methods described in Hart and Blusztajn (2006). TGH3-1931 has 75.1 ppm Rb, 657 ppm Sr, 497 ppm Ba, 76.6 ppm Nb, and ^{87}Sr/^{87}Sr of 0.706467 (normalized to the preferred NBS987 ratio of 0.710240). Tick ("X") marks are 10% mixing increments. The AVON3-71-2 melt inclusion Ba/Nb and ^{87}Sr/^{86}Sr data from this study have a correlation coefficient of 0.81, however the *p*-value for this correlation is only 0.093, indicating the correlation is not significant at the 95% significance level. In (B), the Mauna Loa whole rock ^{87}Sr/^{86}Sr versus Ba/Nb field (from GeoRoc [http://georoc.mpch-mainz.gwdg.de]) compilation, encompasses the Pu'u Wahi melt inclusion analyses from this study; the inset shows a detailed view of Pu'u Wahi melt inclusions from this study.

A simple binary mixing model can be used to generate the heterogeneity observed in the AVON3-71-2 melt inclusions using known whole-rock lava compositions from the Samoan hotspot as hypothetical mixing endmembers. In the model, the geochemically enriched endmember is mixed with a geochemically depleted endmember. We identify two endmembers that are suited for generating the trends exhibited by the melt inclusions (see description of endmembers in Fig. 8 caption). A mixture of these two endmembers generates trends that fit the observed relationships between ^{87}Sr/^{86}Sr and incompatible trace element ratios (e.g. Rb/Sr and Ba/Nb). The observed correlation between trace element ratios (Rb/Sr and Ba/Nb) and ^{87}Sr/^{86}Sr, together with the observation that the AVON3-71-2 melt inclusions fall along the model mixing line, support the hypothesis that the mixing of mantle-derived melts with heterogeneous ^{87}Sr/^{86}Sr prior to eruption could generate the observed ^{87}Sr/^{86}Sr variability.

4.2.2. *Assimilation*

While the mixing of heterogeneous mantle melts could generate the observed ^{87}Sr/^{86}Sr heterogeneity and the concomitant incompatible trace element ratio (Rb/Sr and Ba/Nb) variability, magma mixing alone cannot explain the enrichments in Cl found in the AVON3-71-2 melt inclusions (Fig. 7). The elevated Cl/Nb ratios range up to values (i.e., 33.6) that are above the range for mantle-derived melts, suggesting that assimilation of seawater-derived materials has modified the Cl concentrations of the AVON3-71-2 melt inclusions. However, it is important to evaluate whether the ^{87}Sr/^{86}Sr was modified by this mechanism.

The assimilation of seawater-derived materials—including AOC, seawater, and brines—can modify the ^{87}Sr/^{86}Sr of a melt. This is because seawater-derived materials can have elevated concentrations of Sr and inherit an ^{87}Sr/^{86}Sr ratio from seawater (which contains ~7.85 ppm Sr [Bernat et al., 1972] with radiogenic ^{87}Sr/^{86}Sr [0.709179; Mokadem et al.,

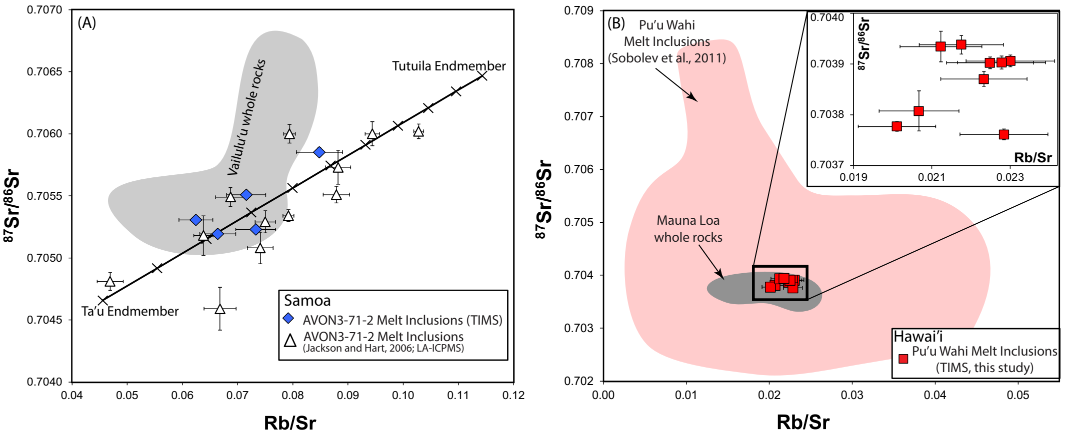

Fig. 9. ^{87}Sr/^{86}Sr versus Rb/Sr for the AVON3-71-2 (A) and Pu'u Wahi (B) melt inclusions. In panel A, the open triangles are data from Jackson and Hart (2006). The black line is a binary mixing line between the two endmembers (samples T10 and TGH-1931, see Fig. 8. caption), and tick ("X") marks are 10% mixing increments. The AVON3-71-2 melt inclusion Rb/Sr and ^{87}Sr/^{86}Sr data from this study give a correlation coefficient of 0.82 with a *p*-value of 0.087. The correlation coefficient of all AVON3-71-2 melt inclusion Rb/Sr and ^{87}Sr/^{86}Sr data from this study and the data of Jackson and Hart (2006) give a correlation coefficient of 0.79 with a *p*-value of 0.0002, indicating the correlation is significant at the 95% significance level. The mixing model describes the melt inclusion data with an R^2 of 0.62; the residuals for our model show no correlation with Rb/Sr (correlation coefficient = −0.08). Vailulu'u whole rock data define a field that encompasses data from Workman et al. (2004) and Jackson et al. (2010). In panel B, the field for Mauna Loa whole rock data encompasses data from the GeoRoc [http://georoc.mpch-mainz.gwdg.de] compilation; a field for melt inclusion analyses from Sobolev et al. (2011) is also shown. The inset shows a detailed view of Pu'u Wahi melt inclusions from this study.

2015]). If olivine crystallizes during or after magmatic assimilation of seawater-altered rock, the melt inclusions would trap signatures of this assimilant.

Several studies have suggested that melt inclusions may be more sensitive recorders of the assimilation of seawater derived materials than whole rock lavas because 1.) crystallization of olivine is enhanced at the magma chamber margins due to cooler temperatures near the magma chamber walls and 2.) melts trapped by growing olivine at magma chamber margins are more likely to have interacted with the wall rock than melts closer to the interior of the chamber (Kamenetsky et al., 1998; Bédard et al., 2000; Danyushevsky et al., 2003, 2004). If assimilation is generating $^{87}Sr/^{86}Sr$ heterogeneity, and if melts hosting signatures of assimilation are preferentially trapped in olivine phenocrysts near magma chamber walls, then variable $^{87}Sr/^{86}Sr$ compositions will be recorded disproportionately in olivine-hosted melt inclusions relative to the bulk lava. This conceptual model may explain the high degree of $^{87}Sr/^{86}Sr$ variability observed in melt inclusions from some lavas.

Identifying signatures of assimilated seawater-derived materials can be difficult due to the geochemical variability in these materials. While the $^{87}Sr/^{86}Sr$ of modern seawater is homogeneous, with a value of 0.709179 (Mokadem et al., 2015), oceanic crust and alteration products can have $^{87}Sr/^{86}Sr$ ratios that range from ~0.7021 in fresh MORB (Schilling et al., 1994; Fontignie and Schilling, 1996) to as high as 0.7257 (Hauff et al., 2003) in highly altered components within early Mesozoic Pacific oceanic crust (where enrichment of Rb in AOC [e.g., Kelley et al., 2003] results in high Rb/Sr that generates high time-integrated $^{87}Sr/^{86}Sr$ via ^{87}Rb decay).

Chlorine provides a powerful tool for identifying assimilation of seawater-derived materials in oceanic lavas because it is fluid mobile and not efficiently subducted into the mantle. Thus, recycled materials in hotspot lavas are not expected to have high Cl/K (e.g., Kendrick et al., 2013) or Cl/Nb (Rowe and Lassiter, 2009), and mantle-derived lavas that have not assimilated seawater-derived materials have low Cl/Nb ratios (e.g. 5–17; Rowe et al., 2015; Michael and Cornell, 1998; Saal et al., 2002; Stroncik and Haase, 2004; Rowe and Lassiter, 2009).

In contrast, seawater and seawater-derived materials (including brines and altered oceanic crust) are rich in Cl (e.g., Sano et al., 2008; Kendrick et al., 2013, 2015; Van den Bleeken and Koga, 2015). Due to alteration by seawater, altered oceanic crust becomes enriched in Cl and other diagnostic elements (including Li, B, K, Rb, Cs, and U; e.g., Kelley et al., 2003; Staudigel, 2003; Sano et al., 2008). However, seawater and brines are poor in Nb relative to mantle-derived melts. As a result, altered oceanic crust inherits high Cl/Nb ratios (and high Cl/K, implied hereafter; Jambon et al., 1995; Michael and Cornell, 1998; Kent et al., 1999a, 1999b, 2002; Lassiter et al., 2002; Kendrick et al., 2013, 2015) relative to mantle-derived melts. Therefore, assimilation of altered oceanic crust by magmas transiting through oceanic crust can elevate the magmatic Cl concentrations relative to similarly incompatible elements, like Nb, resulting in high Cl/Nb ratios in lavas (and melt inclusions) erupted at the surface (e.g., Michael and Cornell, 1998; Kent et al., 1999a, 1999b; Kendrick et al., 2013, 2015).

Therefore, when used in tandem, Cl concentrations and $^{87}Sr/^{86}Sr$ present a powerful tool for evaluating the presence of assimilated seawater derived materials in lavas. Altered oceanic crust has elevated Cl (and Cl/Nb) and higher $^{87}Sr/^{86}Sr$ relative to fresh MORB (Staudigel et al., 1995, 1996; Bach et al., 2003; Hauff et al., 2003; Staudigel, 2003). Thus, if assimilation of seawater derived materials is the mechanism responsible for generating the observed $^{87}Sr/^{86}Sr$ variability in olivine-hosted melt inclusions, then $^{87}Sr/^{86}Sr$ should correlate with indicators of assimilated seawater derived materials (e.g., Cl/Nb). However, Cl and Cl/Nb do not covary with $^{87}Sr/^{86}Sr$ (Fig. 7). This requires that the melt assimilated material that modifies the Cl (and Cl/Nb) of the melt inclusions but does not significantly modify $^{87}Sr/^{86}Sr$. Assimilation of deep crustal gabbros and altered oceanic crust are unlikely candidates (see Supplementary Text). However, as we explain below, interaction with brines may be consistent with the observations of this study.

Kendrick et al. (2015) analyzed Samoan glasses for F, Cl, Br, and I concentrations and reported a Cl/Nb ratio of 32.6 in pillow rim glass from the same lava that we examine here (AVON3-71-2), similar to the Cl/Nb ratio we measured in melt inclusion AVON3-71-2-8 (33.6). Together with evidence from Br and I data, Kendrick et al. (2015) attribute 75% of the Cl in the AVON3-71-2 glass to interaction with brines (totaling 0.45 wt% of the mixture, assuming the brines are composed of 55 ± 15 wt% salts). Other glasses from Vailulu'u (as well as submarine glasses from several other Samoan volcanoes, Ta'u, Malumalu, Tupito [formerly known as Muli], and Taumatau) also exhibit evidence for significant contribution of Cl from brine (Kendrick et al., 2015). Kendrick et al. (2015) and Workman et al. (2006) did not observe a correlation between indicators of assimilation and $^{87}Sr/^{86}Sr$ in the Samoan glasses they analyzed. Kendrick et al. (2013, 2015) suggest that the brine with which the Samoan basalts interacted had low Sr concentrations and therefore interaction with brines could generate the observed Cl enrichment (and high Cl/Nb ratios) without significantly modifying the $^{87}Sr/^{86}Sr$ of the melt.

The influence of melt interacting with brines prior to entrapment can be tested using a simple mixing model. We adopt a 55% salt brine (~30 wt% of the brine is Cl) composition (from Kendrick et al., 2015) that has $^{87}Sr/^{86}Sr$ of seawater (0.709179; Mokadem et al., 2015), a Sr concentration of Mid-Atlantic Ridge hydrothermal fluids (11.1 ppm; Schmidt et al., 2007), and a Nb concentration of 0.2 ppb (le Roux et al., 2006). The brine component is mixed with a melt that has a Cl/Nb ratio equal to the lowest Cl/Nb Vailulu'u glass (sample AVON3-72-2: Cl = 670 ppm, Nb = 67 ppm Cl/Nb = 10.0; Workman et al., 2006) and $^{87}Sr/^{86}Sr$ equal to the lowest $^{87}Sr/^{86}Sr$ inclusion from this study (AVON3-71-2-9; Fig. 7). In our model, a mixture with only 0.52% brine would generate the maximum Cl/Nb (33.6) of the AVON3-71-2 melt inclusions reported here (Fig. 7). This value is similar in magnitude to the 0.45% brine interaction for the AVON3-71-2 pillow glass from Kendrick et al. (2015). Critically, the assimilation of such a small amount of brine increases the $^{87}Sr/^{86}Sr$ ratio of the melt by only 0.5 ppm, more than an order of magnitude less than the uncertainty on the $^{87}Sr/^{86}Sr$ analyses by TIMS reported here. Therefore, interaction with brine can generate elevated Cl/Nb in Vailulu'u melts without significantly modifying the $^{87}Sr/^{86}Sr$ of the melt. Therefore, the lack of correlation between Cl/Nb and $^{87}Sr/^{86}Sr$ in AVON3-71-2 melt inclusions, which host a wide range of Cl/Nb (13.4 to 33.6), is explained by brine interaction with melts prior to entrapment in growing olivines.

Based on the magma mixing model described in Section 4.2.1, binary mixing of geochemically-enriched and geochemically-depleted magmas can generate relationships between $^{87}Sr/^{86}Sr$ and Rb/Sr and Ba/Nb and, critically, none of these ratios are significantly impacted by interaction with brines owing to low Sr, Nb, Rb (Schmidt et al., 2007), and Ba (Charlou et al., 2002) content of brines relative to the alkalic Samoan melts. However, elevated Cl/Nb ratios in the suite of AVON3-71-2 melt inclusions indicate that either (or both) of the endmember magmas in the magma mixing model (Section 4.2.1) interacted with a small amount of brine, variably influencing the melt inclusion Cl budgets (and Cl/Nb ratios) prior to entrapment. Unfortunately, given the existing suite of data, it is not possible to evaluate whether magma mixing or brine interaction occurred first, but the data do suggest that both processes operated on the melts trapped in the AVON3-71-2 melt inclusions.

4.3. Pu'u Wahi (Mauna Loa, Hawai'i)

4.3.1. $^{87}Sr/^{86}Sr$ heterogeneity in melt inclusions from Pu'u Wahi

The Pu'u Wahi melt inclusions analyzed in this study have limited $^{87}Sr/^{86}Sr$ variability (only 251 ppm, 0.703761–0.703938, $N = 9$). However, this limited variability is still greater than the reproducibility of $^{87}Sr/^{86}Sr$ measurements on similarly sized aliquots of Sr (± 43 ppm

2 RSD, based on replicate analyses of 4 ng Sr loads of AGV-1; see Methods), suggesting a very limited range of true Sr-isotopic variability in the suite of Pu'u Wahi melt inclusions examined here. Given the relatively narrow range of $^{87}Sr/^{86}Sr$ ratios, it is difficult to evaluate the mechanisms responsible for generating the $^{87}Sr/^{86}Sr$ variability observed in the Pu'u Wahi melt inclusions analyzed in this study.

The Pu'u Wahi melt inclusions analyzed in this study do not show a correlation between $^{87}Sr/^{86}Sr$ and Cl/Nb (Fig. 7), and they all have low Cl/Nb ratios (< 10.1), so it is unlikely that assimilation of materials altered by seawater is responsible for their limited $^{87}Sr/^{86}Sr$ variability (Lassiter et al., 2002; Workman et al., 2006; Kendrick et al., 2014; Cabral et al., 2014). Additionally, the Pu'u Wahi melt inclusions have Sr/Sr* > 1.2, but there is no relationship between $^{87}Sr/^{86}Sr$ and Sr/Sr* (Fig. S5), which argues against the assimilation of deep oceanic gabbro as the sole mechanism generating the limited $^{87}Sr/^{86}Sr$ heterogeneity (e.g., Saal et al., 2007) (and see Supplementary Information for discussion of gabbro assimilation). Finally, the Pu'u Wahi melt inclusions show no relationship between $^{87}Sr/^{86}Sr$ and Rb/Sr, which excludes simple two-component mixing of magmas as the sole mechanism generating $^{87}Sr/^{86}Sr$ variability in these melt inclusions.

In contrast to the narrow range of $^{87}Sr/^{86}Sr$ ratios obtained on Pu'u Wahi melt inclusions from this study, Sobolev et al. (2011) identified much greater variability (> 30 times greater) in their suite of Pu'u Wahi olivine-hosted melt inclusions (~8500 ppm of $^{87}Sr/^{86}Sr$ variability, 0.7021–0.7081; $N = 137$). The extreme isotopic variability observed by Sobolev et al. (2011) raises some key questions: Why does their dataset exhibit a significantly greater range in $^{87}Sr/^{86}Sr$ in Pu'u Wahi melt inclusions than the dataset generated in this study, and how can we reconcile their results with the relatively narrow range in $^{87}Sr/^{86}Sr$ observed in the melt inclusions in this study?

One possible explanation is that our sample size ($N = 9$ melt inclusions) is significantly smaller than that of Sobolev et al. (2011) ($N = 137$), and the more limited $^{87}Sr/^{86}Sr$ heterogeneity observed in this study (251 ppm) compared to the Sobolev et al. (2011) study (~8500 ppm) is the result of the small sample size. A second possible reason for the contrast between the results of this study and those of Sobolev et al. (2011) is inherent difference in precision between the two analytical methods; the reproducibility of the $^{87}Sr/^{86}Sr$ ratio during repeat $^{87}Sr/^{86}Sr$ analyses of individual Pu'u Wahi melt inclusions by Sobolev et al. (2011) vary considerably, but average errors are ± 1660 ppm (2 RSE) and are as high as ± 4376 ppm (2 RSE, i.e., melt inclusion 1441A in their study). This error is similar to the total range in the Pu'u Wahi melt inclusions suite (~8500 ppm total range) observed by Sobolev et al. (2011). By comparison, the Pu'u Wahi melt inclusions examined here have errors ranging from only ± 14 to ± 56 ppm (2 SE) (and repeat TIMS $^{87}Sr/^{86}Sr$ analyses of 4 ng loads of AGV-1 reproduced to within ± 43 ppm (2 RSD, $N = 6$)). Looking ahead, it will be important to prospect for highly heterogeneous $^{87}Sr/^{86}Sr$ melt inclusions—like those observed in Sobolev et al.'s (2011) study—in a larger suite of Pu'u Wahi melt inclusions using the TIMS technique employed here. Additionally, multiple clasts of the Pu'u Wahi eruption should be examined as significant variability in olivine forsterite content has been observed between clasts of the Pu'u Wahi eruption (Wallace et al., 2015).

4.4. Conclusions

In this study, we present the first paired $^{87}Sr/^{86}Sr$ and $^{143}Nd/^{144}Nd$ data on individual olivine-hosted melt inclusions from OIB lavas from Hawai'i (sample from the Pu'u Wahi eruption of Mauna Loa) and Samoa (from Vailulu'u volcano). The combination of isotopic and trace-element analyses on individual olivine-hosted melt inclusions allows the identification of processes that can modify mantle melts prior to eruption. In the suite of melt inclusions from the Samoa AVON3-71-2 lava, we report 936 ppm variability in $^{87}Sr/^{86}Sr$ in six melt inclusions, and these new data (obtained using a TIMS technique) represent 46% of the variability in $^{87}Sr/^{86}Sr$ reported on a different suite of 12 melt inclusions from this lava analyzed by LA-MC-ICP-MS (Jackson and Hart, 2006). For the Samoan melt inclusions, we show that the mixing of isotopically heterogeneous mantle-derived melts may be an important mechanism generating the observed $^{87}Sr/^{86}Sr$ heterogeneity, and that localized interaction with small amounts ($< 1\%$) of brine generates the observed Cl enrichments and high Cl/Nb ratios (up to 33.6). The relatively homogeneous $^{87}Sr/^{86}Sr$ in Pu'u Wahi melt inclusions obtained by TIMS (251 ppm variability in $^{87}Sr/^{86}Sr$ on nine melt inclusions) identified here contrasts with previously reported extreme $^{87}Sr/^{86}Sr$ variability (~8500 ppm variability in $^{87}Sr/^{86}Sr$ on 137 melt inclusions) in melt inclusions from the same eruption using a single-collector LA-ICP-MS technique. We were able to show that heterogeneous $^{87}Sr/^{86}Sr$ in Samoan melt inclusions using LA-MC-ICP-MS can be replicated using a TIMS technique (this study and Reinhard et al., 2016). Therefore, it will be important to employ a TIMS technique to confirm the highly heterogeneous (and extremely radiogenic) $^{87}Sr/^{86}Sr$ compositions identified in Pu'u Wahi melt inclusions by Sobolev et al. (2011), but on a larger suite of melt inclusions than was analyzed in this study.

Acknowledgements

We thank E. Gazel and an anonymous reviewer for constructive reviews, and C. Chauvel for editorial handling. MGJ acknowledges NSF grants OCE-1736984 and EAR-1624840. AAR gratefully acknowledges support from Ken MacDonald and Rachel Haymon through the UCSB Earth Science Department Graduate Opportunity Award which made this work possible. EFR-K acknowledges the partial financial support by the French Government Laboratory of Excellence initiative no. ANR-10-LABX-0006, the Region Auvergne, and the European Regional Development Fund. This is Laboratory of Excellence ClerVolc (contribution number 319). JMK recieved funding from the European Research Council (ERC) under the European Union's Horizon 2020 research and innovation program (grant agreement No 654208 Europlanet 2020 RI).

Appendix A. Supplementary data

Supplementary data to this article can be found online at https://doi.org/10.1016/j.chemgeo.2018.07.034.

References

Bach, W., Peucker-Ehrenbrink, B., Hart, S.R., Blusztjan, J.S., 2003. Geochemistry of hydrothermally altered oceanic crust: DSDP/ODP Hole 504B – implications for seawater-crust exchange budgets and Sr- and Pb-isotopic evolution of the mantle. Geochem. Geophys. Geosyst. 4 (3). https://doi.org/10.1029/2002GC000419.

Beattie, P., 1994. Systematics and energetics of trace-element partitioning between olivine and silicate melts: implications for the nature of mineral/melt partitioning. Chem. Geol. 117, 57–71.

Bédard, J.H., Hébert, R., Berclaz, A., Varfalvy, V., 2000. Syntexis and the genesis of lower oceanic crust. In: Dilek, Y., Moores, E.M., Elthon, D., Nicolas, A. (Eds.), Ophiolites and Oceanic Crust: New Insights From Field Studies and the Ocean Drilling Program. vol. 349. Geol. Soc. America, Boulder, Colorado, Spec. Pap, pp. 105–119.

Bernat, M., Church, T., Allègre, C.J., 1972. Barium and strontium concentrations in Pacific and Mediterranean sea water profiles by direct isotope dilution mass spectrometry. Earth Planet. Sci. Lett. 16, 75–80.

Borisova, A.Y., Faure, F., Deloule, E., Grègoire, M., Bèjina, F., de Parseval, Ph., Devidal, J.-L., 2014. Lead isotope signatures of Kerguelen plume-derived olivine hosted melt inclusions: constraints on the ocean island basalt petrogenesis. Lithos 198–199, 153–171. https://doi.org/10.1016/j.lithos.2014.03.022.

Bryce, J.G., DePaolo, D.J., 2004. Pb isotopic heterogeneity in basaltic phenocrysts. Geochim. Cosmochim. Acta 68, 4453–4468.

Cabral, R.A., Jackson, M.G., Rose-Koga, E.F., Koga, K.T., Whitehouse, M.J., Antonelli, M.A., Farquhar, J., Day, J.M.D., Hauri, E.H., 2013. Anomalous sulphur isotopes in plume lavas reveal deep mantle storage of Archaean crust. Nature 496, 490–493.

Cabral, R.A., Jackson, M.G., Koga, K.T., Rose-Koga, E.F., Hauri, E.H., Whitehouse, M.J., Price, A.A., Day, J.M.D., Shimizu, N., Kelley, K.A., 2014. Volatile cycling of H_2O, CO_2, F, and Cl in the HIMU mantle: a new window provided by melt inclusions from oceanic hotspot lavas at Mangaia, Cook Islands. Geochem. Geophys. Geosyst. 15. https://doi.org/10.1002/2014GC005473.

Carlson, R.W., 1994. Mechanisms of earth differentiation - consequences for the chemical structure of the mantle. Rev. Geophys. 32, 337–361.

Charlou, J.L., Donval, J.P., Fouquet, Y., Jean-Baptiste, P., Holm, N., 2002. Geochemistry of high H_2 and CH_4 vent fluids issuing from ultramafic rocks at Rainbow hydrothermal field (36° 14′N, MAR). Chem. Geol. 191, 345–359.

Danyushevsky, L.V., Sobolev, A.V., Kononkova, N.N., 1992. Methods of studying melt inclusions in minerals during investigations on water-bearing primitive mantle melts (Tonga Trench boninites). Geochem. Int. 29, 48–62.

Danyushevsky, L.V., Della-Pasqua, F.N., Sokolov, S., 2000. Re-equilibration of melt inclusions trapped by magnesian olivine phenocrysts from subduction-related magmas: petrological implications. Contrib. Mineral. Petrol. 138, 68–83.

Danyushevsky, L.V., Perfit, M.R., Eggins, S.M., Falloon, T.J., 2003. Crustal origin for coupled ‘ultra-depleted’ and ‘plagioclase’ signatures in MORB olivine-hosted melt inclusions: evidence from the Siqueiros Transform Fault, East Pacific Rise. Contrib. Mineral. Petrol. 144, 619–637.

Danyushevsky, L.V., Leslie, R.A.J., Crawford, A.J., Durance, P., 2004. Melt inclusions in primitive olivine phenocrysts: the role of localized reaction processes in the origin of anomalous compositions. J. Petrol. 45, 2531–2553.

DePaolo, D., Wasserburg, G.J., 1976. Inferences about magma sources and mantle structure from variations of ^{143}Nd/^{144}Nd. Geophys. Res. Lett. 3, 743–746.

Fontignie, D., Schilling, J.G., 1996. Mantle heterogeneities beneath the South Atlantic: a Nd–Sr–Pb isotope study along the Mid-Atlantic Ridge (3°S–46°S). Earth Planet. Sci. Lett. 142, 209–221.

Ford, C.E., Russel, D.G., Craven, J.A., Fisk, M.R., 1983. Olivine-liquid equilibria: temperature, pressure and composition dependence of the crystal/liquid cation partition coefficients for Mg, Fe^{2+}, Ca and Mn. J. Petrol. 24, 256–265.

Fujimaki, H., Tatsumoto, M., Aoki, K-i., 1984. Partition coefficients of Hf, Zr, and REE between phenocrysts and groundmasses. J. Geophys. Res. 89, 662–672.

Gaetani, G.A., Watson, E.B., 2000. Open system behavior of olivine hosted melt inclusions. Earth Planet. Sci. Lett. 183, 27–41.

Gaetani, G.A., O'Leary, J.A., Shimizu, N., Bucholz, C.E., Newville, M., 2012. Rapid reequilibration of H_2O and oxygen fugacity in olivine-hosted melt inclusions. Geology 40, 915–918. https://doi.org/10.1130/G32992.1.

Gagnon, J.E., Fryer, B.J., Samson, I.M., Williams-Jones, A.E., 2008. Quantitative analysis of silicate certified reference materials by LA-ICPMS with and without an internal standard. J. Anal. At. Spectrom. 23, 1529–1537.

Gast, P.W., Tilton, G.R., Hedge, C., 1964. Isotopic composition of lead and strontium from Ascension and Gough Islands. Science 145, 1181–1185.

Gurenko, A.A., Chaussidon, M., 1995. Enriched and depleted primitive melts in olivine from Icelandic tholeiites: origin by continuous melting of a single mantle column. Geochim. Cosmochim. Acta 59, 2905–2917.

Hamelin, C., Dosso, L., Hanan, B., Moreira, M., Kositsky, A.P., Thomas, M.Y., 2011. Geochemical portray of the Pacific ridge: new isotopic data and statistical techniques. Earth Planet. Sci. Lett. 302, 154–162.

Harlou, R., Pearson, D.G., Nowell, G.M., Ottley, C.J., Davidson, J.P., 2009. Combined Sr isotope and trace element analysis of melt inclusions at sub-ng levels using micromilling, TIMS and ICPMS. Chem. Geol. 260, 254–268.

Hart, S.R., Blusztajn, J., 2006. Age and geochemistry of the mafic sills, ODP site 1276, Newfoundland margin. Chem. Geol. 235, 222–237.

Hauff, F., Hoernle, K., Schmidt, A., 2003. Sr-Nd-Pb composition of Mesozoic Pacific oceanic crust (Site 1149 and 801, ODP Leg 185): implications for alteration of ocean crust and the input into the Izu-Bonin-Mariana subduction system. Geochem. Geophys. Geosyst. 4, 8913. https://doi.org/10.1029/2002GC000421.

Hofmann, A.W., 1997. Mantle geochemistry: the message from oceanic volcanism. Nature 385, 219–229.

Hofmann, A.W., White, W.M., 1982. Mantle plumes from ancient oceanic crust. Earth Planet. Sci. Lett. 57, 421–436.

Jackson, M.G., Hart, S.R., 2006. Strontium isotopes in melt inclusions from Samoan basalts: implications for heterogeneity in the Samoan plume. Earth Planet. Sci. Lett. 245, 260–277.

Jackson, M.G., Shirey, S., 2011. Re-Os systematics in Samoan shield lavas and the use of Os-isotopes in olivine phenocrysts to determine primary magmatic compositions. Earth Planet. Sci. Lett. 312, 91–101.

Jackson, M.G., Hart, S.R., Shimizu, N., Blusztajn, J., 2009. Pervasive cpx-whole rock isotopic disequilibrium in Polynesian hotspot lavas: evidence supporting isotopic variability in olivine and clinopyroxene-hosted melt inclusions. Geochem. Geophys. Geosyst. 10, Q03006. https://doi.org/10.1029/2008GC002324.

Jackson, M.G., Hart, S.R., Konter, J.P., Koppers, A.A.P., Staudigel, H., Kurz, M.D., Blusztajn, J., Sinton, J.M., 2010. The Samoan hotspot track on a “hotspot highway”: implications for mantle plumes and a deep Samoan mantle source. Geochem. Geophys. Geosyst. 11, Q12009. https://doi.org/10.1029/2010GC003232.

Jackson, M.G., Hart, S.R., Konter, J.G., Kurz, M.D., Blusztajn, J., Farley, K., 2014. Helium and lead isotopes reveal the geochemical geometry of the Samoan plume. Nature 514, 355–358.

Jambon, A., Deruelle, B., Dreibus, G., Pineau, F., 1995. Chlorine and bromine abundance in MORB: the contrasting behaviour of the Mid-Atlantic Ridge and East Pacific Rise and implications for chlorine geodynamic cycle. Chem. Geol. 126, 101–117.

Jochum, K., Stoll, B., Herwig, K., Willbold, M., Hofmann, A., Amini, M., Aarburg, S., Abouchami, W., Hellebrand, E., Mocek, B., Raczek, I., Stracke, A., Alard, O., Bouman, C., Becker, S., Dücking, M., Brätz, H., Klemd, R., Bruin, D., Canil, D., Cornell, D., Hoog, C.-J., Dalpe, C., Danyushevsky, L., Eisenhauer, A., Gao, Y., Snow, J., Groschopf, N., Günther, D., Latkoczy, C., Guillong, M., Hauri, E., Höfer, H., Lahaye, Y., Horz, K., Jacob, D., Kasemann, S., Kent, A., Ludwig, T., Zack, T., Mason, P., Meixner, A., Rosner, M., Misawa, K., Nash, B., Pfänder, J., Premo, W., Sun, W., Tiepolo, M., Vannucci, R., Vennemann, T., Wayne, D., Woodhead, J., 2006. MPI-DING reference glasses for in situ microanalysis: new reference values for element concentrations and isotope ratios. Geochem. Geophys. Geosyst. 7.

Kamenetsky, V.S., Eggins, S.M., Crawford, A.J., Green, D.H., Gasparon, M., Falloon, T.J., 1998. Calcic melt inclusions in primitive olivine at 43° N MAR: evidence for melt–rock reaction/melting involving clinopyroxene-rich lithologies during MORB generation. Earth Planet. Sci. Lett. 160, 115–132.

Kelley, K.A., Plank, T., Ludden, J., Staudigel, H., 2003. Composition of altered oceanic crust at ODP Sites 801 and 1149. Geochem. Geophys. Geosyst. 4. https://doi.org/10.1029/2002GC000435.

Kelley, K.A., Kingsley, R., Schilling, J.-G., 2013. Composition of plume-influenced mid-ocean ridge lavas and glasses from the Mid-Atlantic Ridge, East Pacific Rise, Galapagos Spreading Center, and Gulf of Aden. Geochem. Geophys. Geosyst. 14, 223–242. https://doi.org/10.1029/2012GC004415.

Kendrick, M.A., Arculus, R., Burnard, P., Honda, M., 2013. Quantifying brine assimilation by submarine magmas: examples from the Galapagos Spreading Centre and Lau Basin. Geochim. Cosmochim. Acta 123, 150–165. https://doi.org/10.1016/j.gca.2013.09.012.

Kendrick, M.A., Jackson, M.G., Kent, A.J.R., Hauri, E.H., Wallace, P.J., Woodhead, J., 2014. Contrasting behaviors of CO_2, S, H_2O and halogens (F, Cl, Br, and I) in enriched- mantle melts from Pitcairn and Society seamounts. Chem. Geol. 370, 69–81.

Kendrick, M.A., Jackson, M.G., Hauri, E.H., Phillips, D., 2015. The halogen (F, Cl, Br, I) and H_2O systematics of Samoan lavas: assimilated-seawater, EM2 and high-^{3}He/^{4}He components. Earth Planet. Sci. Lett. 410, 197–209.

Kent, A.J.R., 2008. Melt inclusions in basaltic and related volcanic rocks. Rev. Mineral. Geochem. 69, 273–331.

Kent, A.J., Norman, M.D., Hutcheon, I.D., Stolper, E.M., 1999a. Assimilation of seawater-derived components in an oceanic volcano: evidence from matrix glasses and glass inclusions from Loihi seamount, Hawai'i. Chem. Geol. 156, 299–319.

Kent, A.J., Clague, D.A., Honda, M., Stolper, E.M., Hutcheon, I.D., Norman, M.D., 1999b. Widespread assimilation of a seawater-derived component at Loihi Seamount, Hawai'i. Geochim. Cosmochim. Acta 63, 2749–2761.

Kent, A.J.R., Baker, J.A., Wiedenbeck, M., 2002. Contamination and melt aggregation processes in continental flood basalts: constraints from melt inclusions in Oligocene basalts from Yemen. Earth Planet. Sci. Lett. 202, 577–594.

Knaf, A.C.S., Koornneef, J.M., Davies, G.R., 2017. “Non-invasive” portable laser ablation sampling of art and archaeological materials with subsequent Sr–Nd isotope analysis by TIMS using 10^{13} Ω amplifiers. J. Anal. At. Spectrom. 32, 2210–2216.

Koornneef, J.M., Bouman, C., Schwieters, J.B., Davies, G.R., 2014. Measurement of small ion beams by thermal ionization mass spectrometry using new 10^{13} Ohm resistors. Anal. Chim. Acta 819, 49–55.

Koornneef, J.M., Nikogosian, I., van Bergen, M.J., Smeets, R., Bouman, C., Davies, G.R., 2015. TIMS analysis of Sr and Nd isotopes in melt inclusions from Italian potassium-rich lavas using prototype 10^{13} Ω amplifiers. Chem. Geol. 397, 14–23.

Lassiter, J.C., Hauri, E.H., Nikogosian, I.K., Barsczus, H.G., 2002. Chlorine–potassium variations in melt inclusions from Raivavae and Rapa, Austral Islands: constraints on chlorine recycling in the mantle and evidence for brine-induced melting of oceanic crust. Earth Planet. Sci. Lett. 202, 525–540.

le Roux, P.J., Shirey, S.B., Hauri, E.H., Perfit, M.R., Bender, J.F., 2006. The effects of variable sources, processes and contaminants on the composition of northern EPR MORB (8–10°N and 12–14°N): evidence from volatiles (H_2O, CO_2, S) and halogens (F, Cl). Earth Planet. Sci. Lett. 251, 209–231.

Le Voyer, M., Rose-Koga, E.F., Laubier, M., Schiano, P., 2008. Petrogenesis of arc lavas from the Rucu Pichincha and Pan de Azucar volcanoes (Ecuadorian arc): major, trace element, and boron isotope evidences from olivine-hosted melt inclusions. Geochem. Geophys. Geosyst. 9. https://doi.org/10.1029/2008GC002173.

Lockwood, J.P., 1995. Mauna Loa eruptive history: the preliminary radiocarbon record. In: Rhodes, J.M., Lockwood, J.P. (Eds.), Mauna Loa Revealed: Structure, Composition, History, and Hazards. Vol. 92. American Geophysical Union Geophysical Monograph, pp. 81–94. https://doi.org/10.1029/GM092p0081.

Maclennan, J., 2008. Lead isotope variability in olivine-hosted melt inclusions from Iceland. Geochim. Cosmochim. Acta 72, 4159–4176.

Maclennan, J., McKenzie, D., Granvöld, K., Shimizu, N., Eiler, J.M., Kitchen, N., 2003a. Melt mixing and crystallization under Theistareykir, northeast Iceland. Geochem. Geophys. Geosyst. 4. https://doi.org/10.1029/2003GC000558.

Maclennan, J., McKenzie, D., Hilton, D., Granvöld, K., Shimizu, N., 2003b. Geochemical variability in a single flow from northern Iceland. J. Geophys. Res. 108, 2007.

McDonough, W.F., Sun, S.S., 1995. The composition of the Earth. Chem. Geol. 120, 223–253.

Melson, W.G., O'Hearn, T., Jarosewich, E., 2002. A data brief on the Smithsonian Abyssal Volcanic Glass Data File. Geochem. Geophys. Geosyst. 3 (4), 1023. https://doi.org/10.1029/2001GC000249.

Michael, P.J., Cornell, W.C., 1998. Influence of spreading rate and magma supply on crystallization and assimilation beneath mid-ocean ridges: evidence from chlorine and major element chemistry of mid-ocean ridge basalts. J. Geophys. Res. 103, 18,325–18,356.

Mokadem, F., Parkinson, I.J., Hathorne, E.C., Anand, P., Allen, J.T., Burton, K.W., 2015. High-precision radiogenic strontium isotope measurements of the modern and glacial ocean: limits on glacial–interglacial variations in continental weathering. Earth Planet. Sci. Lett. 415, 111–120.

Oulton, J., Humayun, M., Fedkin, A., Grossman, L., 2016. Chemical evidence for differentiation, evaporation and recondensation from silicate clasts in Gujba. Geochim. Cosmochim. Acta 177, 254–274.

Ramos, F.C., Wolff, J.A., Tollstrup, D.L., 2004. Measuring ^{87}Sr/^{86}Sr variations in minerals and groundmass from basalts using LA-MC-ICPMS. Chem. Geol. 211, 135–158.

Reinhard, A.A., Jackson, M.G., Harvey, J., Brown, C., Koornneef, J.M., 2016. Extreme differences in ^{87}Sr/^{86}Sr between magmatic olivines and Samoan host lavas: evidence for highly heterogeneous ^{87}Sr/^{86}Sr in the magmatic plumbing system sourcing a single lava. Chem. Geol. 438, 120–131.

Remmert, P., Dohmen, R., Chakraborty, S., 2008. Diffusion of REE, Hf and Sr in olivine. Eos. Trans. AGU 89 (53) (Fall Meet. Suppl. MR33A-1844 (abstr.)).

Roeder, P.L., Emslie, R.F., 1970. Olivine–liquid equilibrium. Contrib. Mineral. Petrol. 29, 275–289.

Rose-Koga, E.F., Koga, K., Schiano, P., Le Voyer, M., 2012. Mantle source heterogeneity for South Tyrrhenian magmas revealed by Pb isotopes and halogen contents of olivine-hosted melt inclusions. Chem. Geol. 334, 266–279.

Rose-Koga, E., Koga, K., Moreira, M., Vlastélic, I., Jackson, M.G., Whitehouse, M.J., Shimizu, N., Habib, N., 2017. Geochemical systematics of Pb isotopes, fluorine, and sulfur in melt inclusions from São Miguel, Azores. Chem. Geol. 458, 22–37. https://doi.org/10.1016/j.chemgeo.2017.03.024.

Rowe, M.C., Lassiter, J.C., 2009. Chlorine enrichment in central Rio Grande Rift basaltic melt inclusions: evidence for subduction modification of the lithospheric mantle. Geology 37, 439–442.

Rowe, M.C., Lassiter, J.C., Goff, K., 2015. Basalt volatile fluctuations during continental rifting: an example from the Rio Grande Rift, USA. Geochem. Geophys. Geosyst. 16. https://doi.org/10.1002/2014GC005649.

Saal, A.E., Hart, S.R., Shimizu, N., Hauri, E.H., Layne, G.D., 1998. Pb isotopic variability in melt inclusions from oceanic island basalts, Polynesia. Science 282, 1481–1484.

Saal, A.E., Hauri, E.H., Langmuir, C.H., Perfit, M.R., 2002. Vapour undersaturation in primitive mid-ocean-ridge basalt and the volatile content of Earth's upper mantle. Nature 419, 451–455.

Saal, A.E., Hart, S.R., Shimizu, N., Hauri, E.H., Layne, G.D., Eiler, J.M., 2005. Pb isotopic variability in melt inclusions from the EMI-EMII-HIMU mantle end-members and the role of oceanic lithosphere. Earth Planet. Sci. Lett. 240, 605–620.

Saal, A.E., Kurz, M.D., Hart, S.R., Blusztajn, J.S., Blichert-Toft, J., Liang, Y., Geist, D.J., 2007. The role of lithospheric gabbros on the composition of Galapagos lavas. Earth Planet. Sci. Lett. 257 (3–4), 391–406.

Sakyi, P.A., Tanaka, R., Kobayashi, K., Nakamura, E., 2012. Inherited Pb isotopic record in olivine antecryst-hosted melt inclusions from Hawai'ian lavas. Geochim. Cosmochim. Acta 95, 169–195.

Salters, V.J.M., Mallick, S., Hart, S.R., Langmuir, C.E., Stracke, A., 2011. Domains of depleted mantle: new evidence from hafnium and neodymium isotopes. Geochem. Geophys. Geosyst. 12, Q08001. https://doi.org/10.1029/2011GC003617.

Sano, T., Miyoshi, M., Ingle, S., Banerjee, N.R., Ishimoto, M., Fukuoka, T., 2008. Boron and chlorine contents of upper oceanic crust: basement samples from IODP Hole 1256D. Geochem. Geophys. Geosyst. 9, Q12O15. https://doi.org/10.1029/2008GC002182.

Schilling, J.G., Hanan, B.B., McCully, B., Kingsley, R.H., Fontignie, D., 1994. Influence of the Sierra Leone mantle plume on the equatorial Mid-Atlantic Ridge: a Nd-Sr-Pb isotopic study. J. Geophys. Res. 99 (B6), 12,005–12,028. https://doi.org/10.1029/94JB00337.

Schmidt, K., Koschinsky, A., Garbe-Schönberg, D., de Carvalho, L.M., Seifert, R., 2007. Geochemistry of hydrothermal fluids from the ultramafic-hosted Logatchev I hydrothermal field, 15°N on the Mid-Atlantic Ridge: temporal and spatial investigation. Chem. Geol. 242 (1–2), 1–21. https://doi.org/10.1016/j.chemgeo.2007.01.023.

Sims, K.W.W., Hart, S.R., Reagan, M.K., Blusztajn, J., Staudigel, H., Sohn, R.A., Layne, G.D., Ball, L.A., 2008. ^{238}U-^{230}Th-^{226}Ra-^{210}Pb-^{210}Po, ^{232}Th-^{228}Ra, and ^{235}U-^{231}Pa constraints on the ages and petrogenesis of Vailulu'u and Malumalu Lavas, Samoa. Geochem. Geophys. Geosyst. 9, Q04003. https://doi.org/10.1029/2007GC001651.

Sobolev, A.V., Danyushevsky, L.V., 1994. Petrology and geochemistry of boninites from the north termination of the Tonga Trench: constraints on the generation conditions of primary high-Ca boninite magmas. J. Petrol. 35, 1183–1213.

Sobolev, A.V., Shimizu, N., 1993. Ultra-depleted primary melt included in an olivine from the mid-Atlantic ridge. Nature 363, 151–154.

Sobolev, A.V., Hofmann, A.W., Nikogosian, I.K., 2000. Recycled oceanic crust observed in 'ghost plagioclase' within the source of Mauna Loa lavas. Nature 404, 986–990.

Sobolev, A.V., Hofmann, A.W., Jochum, K.P., Kuzmin, D.V., Stoll, B., 2011. A young source for the Hawai'ian plume. Nature 476, 434–437.

Staudigel, H., 2003. Hydrothermal alteration processes in the Oceanic Crust. In: Treatise on Geochemistry. vol. 3. pp. 511–535.

Staudigel, H., Davies, G.R., Hart, S.R., Marchant, K.M., Smith, B.M., 1995. Large scale isotopic Sr, Nd and O isotopic anatomy of altered oceanic crust: DSDP/ODP sites 417/418. Earth Planet. Sci. Lett. 130, 169–185.

Staudigel, H., Plank, T., White, B., Schminke, H.-U., 1996. Geochemical fluxes during seafloor alteration of the basaltic upper oceanic crust: DSDP Sites 417 and 418. In: Bebout, G.E. (Ed.), Subduction: Top to Bottom, Geophys. Monogr. Ser. vol. 96. AGU, Washington, D.C., pp. 19–38 (1996).

Stracke, A., 2016. Mantle geochemistry. In: Encyclopedia of Geochemistry, pp. 12. https://doi.org/10.1007/978-3-319-39193-9_286–1.

Stroncik, N.A., Haase, K.M., 2004. Chlorine in oceanic intraplate basalts: constraints on mantle sources and recycling processes. Geology 32, 945–948. https://doi.org/10.1130/G21027.1.

Sun, S.S., McDonough, W.F., 1989. Chemical and isotopic systematic of oceanic basalts: implications for mantle composition and processes. In: Saunders, A.D., Norry, M.J. (Eds.), Magmatism in the Ocean Basins. vol. 42. Geological Society Special Publications, pp. 313–345.

Tanaka, T., Togashi, S., Kamioka, H., Dragusanu, C., 2000. JNdi-1: a neodymium isotopic reference in consistency with La Jolla neodymium. Chem. Geol. 168, 279–281.

Thirlwall, M.F., 1991. Long-term reproducibility of multicollector Sr and Nd isotope ratio analysis. Chem. Geol. 94, 85–104.

Van den Bleeken, G., Koga, K.T., 2015. Experimentally determined distribution of fluorine and chlorine upon hydrous slab melting, and implications for F–Cl cycling through subduction zones. Geochim. Cosmochim. Acta 171, 353–373.

Vroon, P.Z., van der Wagt, B., Koornneef, J.M., Davies, G.R., 2008. Problems in obtaining precise and accurate Sr isotope analysis from geological materials using laser ablation MC-ICPMS. Anal. Bioanal. Chem. 390, 465–476.

Wallace, P.J., Kamenetsky, V.S., Cervantes, P., 2015. Melt inclusion CO$_2$ contents, pressures of olivine crystallization, and the problem of shrinkage bubbles. Am. Mineral. 100 (4), 787–794.

Weis, D., Kieffer, B., Maerschalk, C., Barling, J., Jong, J.D., Williams, G.A., Hanano, D., Pretorius, W., Mattielli, N., Scoates, J.S., Goolaerts, A., Friedman, R.M., Mahoney, J.B., 2006. High precision isotopic characterization of USGS reference materials by TIMS and MC-ICP-MS. Geochem. Geophys. Geosyst. 7 (8), 139–149.

White, W.M., 1985. Source of oceanic basalts: radiogenic isotopic evidence. Geology 13, 115–118.

White, W.M., 2010. Oceanic Island Basalts and mantle plumes: the geochemical perspective. Annu. Rev. Earth Planet. Sci. 38, 133–160.

White, W.M., 2015a. Isotopes, DUPAL, LLSVPs, and Anekantavada. Chem. Geol. 419, 10–28.

White, W.M., 2015b. Probing the Earth's deep interior through geochemistry. Geochem. Perspect. 4 (2), 95–251.

Workman, R.K., Hart, S.R., Jackson, M.G., Regelous, M., Farley, K.A., Blusztajn, J., Kurz, M.D., 2004. Recycled metasomatised lithosphere as the origin of the Enriched Mantle II (EM2) end-member: evidence from the Samoan Volcanic Chain. Geochem. Geophys. Geosyst. https://doi.org/10.1029/2003GC000623. (5gao).

Workman, R.K., Hauri, E., Hart, S.R., Wang, J., Blusztajn, J., 2006. Volatile and trace elements in basaltic glasses from Samoa: implications for water distribution in the mantle. Earth Planet. Sci. Lett. 241, 932–951.

Workman, R.K., Hart, S.R., Eiler, J.M., Jackson, M.G., 2008. Oxygen isotopes in Samoan lavas: confirmation of continent recycling. Geology 36, 551–554.

Yurimoto, H., Kogiso, T., Abe, K., Barsczus, H.G., Utsunomiya, A., Maruyama, S., 2004. Lead isotopic compositions in olivine-hosted melt inclusions from HIMU basalts and possible link to sulfide components. Phys. Earth Planet. Inter. 146 (1–2), 231–242. https://doi.org/10.1016/j.pepi.2003.08.013.

Zindler, A., Hart, S.R., 1986. Chemical geodynamics. Annu. Rev. Earth Planet. Sci. 14, 493–571.